The role of Mitogen Activated Protein Kinase (MAPK) Phosphatases (MKPs) in adipogenesis

A study of *Vaccinia* H1-related (VHR) phosphatase

Jørgen Sikkeland

Thesis for the Master of Science degree in Molecular Biology

Department of Molecular Biosciences, Faculty of Mathematics and Natural Sciences

UNIVERSITETET OF OSLO

June 2008

Acknowledgements

The present work was carried out from January 2007 to June 2008 in the laboratory of Professor Fahri Saatcioglu at the Department of Molecular Biosciences, University of Oslo.

I would like to thank my main supervisor Fahri Saatcioglu for having created a great arena for research and letting me be a part of it. Throughout the master-project he has given me valuable inputs on being a scientist and the time I needed to find my own drive for research. I will especially remember that creativity comes with knowledge.

A special thanks to Torstein Lindstad, my other supervisor, for always being willing to discuss and never letting me forget that there is always more than one way to look at an issue. I would like to give both my supervisors credit for all the help during the writing process.

Thanks to the rest of the group for a good working environment, nice cakes and fun times with the radio.

A cheer to my fellow students for adding a social context to studying at the university and to my friends back home for giving me a shelter when I got fed up with Oslo.

Last, but not least, thanks to my brother and sister for being who they are and my parents for making me who I am.

Oslo, June 2008

Jørgen Sikkeland

Abstract

Animals store most excess energy as fat in specialized cells called adipocytes which form the major part of adipose tissue. Since obesity, which has reached epidemic proportions in the last decades, is the result of excess growth of the adipose tissue caused by both hypertrophy and hyperplasia, understanding how adipocytes expand is an important area research. Adipogenesis, the development of progenitor cells to mature adipocytes, has been widely studied with mouse models and in particular with differentiation of the murine preadipocytes 3T3-L1 and 3T3-F22A. Previous research has found Mitogen Activated Protein kinase (MAPK) activity to be required in the early stages of adipogenesis. MKPs are phosphatases with MAPKs as their substrate. They are known to dephosphorylate MAPKs in several tissues. MKP1 has been shown to have a role in adipogenesis as it can regulate phosphorylation of the MAPK ERK in differentiating 3T3-L1 cells. Previous findings in our group have shown many MKPs to be regulated at the mRNA level during 3T3-L1 differentiation; one of these, MKP5, has been shown to enhance adipocyte differentiation when ectopically expressed. In this study we found that one of the other MKPs, *Vaccinia* H1-related (VHR) phosphatase is regulated during adipogenesis. We also validate the integrity of two kinds of expression vector constructs created for three MKPs (VHR, MKP6 and VH5) all of which have been shown to be regulated during adipogenesis. The vector constructs for VHR were used in characterization of its potential role in differentiation of 3T3-L1 cells. These results further underscore the importance of MKPs in adipogenesis and pave the way for future studies.

Abbreviations

AC	adenylyl cyclase
aP2	adipocyte fatty acid binding protein 2
ATGL	adipose triglyceride lipase
BAT	brown adipose tissue
BBB	blood brain barrier
BMI	body mass index
C/EBP	CCAAT/enhancer binding protein
CNS	central nervous system
Dox	doxycycline
DUSP	dual specificity phosphatases
ERK	extracellular signal-regulated kinase
FATP	fatty acid transporter protein
FFA	free fatty acid
GLUT4	glucose transporter 4
HSL	hormone-sensitive lipase
IGF-IR	insulin like growth factor insulin receptor
IL-6	interleukin 6
IR	insulin receptor
JAK	Janus kinase
JNK	c-Jun N-terminal kinase
LPL	lipoprotein lipase
MAP2K	MAPK kinase
MAP3K	MAPK kinase kinase
MAPK	mitogen activated protein kinase
MCE	mitotic clonal expansion
MCP-1	monocyte chemoattractant protein 1
MKP	MAPK phosphatase
MSC	mesenchymal stem cell
Ob	gene that codes for leptin
PAI-1	plasminogen activator inhibitor-1
PDE	phosphodiesterase
PKA	protein kinase A
PKB	protein kinase B
PPAR	peroxisome proliferator-activated receptor
rtTA	reverse tetracycline-controlled transactivator
SOCS3	suppressor of cytokine signaling 3
STAT	signal transducer and activator of transcription
Tc	tetracycline
TG	triacylglycerol
TNFα	tumor necrosis factor alfa
UCP1	uncoupling protein-1
VHR	*Vaccinia* H1-related (VHR) phosphatase
WAT	white adipose tissue

Contents

1. Introduction

1.1 Adipose tissue

Animals store most excess energy as fat in the form of triacylglycerol (TG). Most TG is stored in specialized cells, called adipocytes, which are the main cell type of adipose tissue. Although there are differences among species, the basic concepts of adipose anatomy and physiology are similar between the commonly studied small rodents and less studied larger mammals, including humans [1].

The adipose tissue is a loose connective tissue organized in separate depots. Each depot has their own supply of blood vessels, lymph nodes and nerves. The adipose tissue is separated into two main groups. Visceral adipose tissue is located inside the thorax and abdomen in relation to other organs while the main subcutaneous depots lie in the anterior and posterior part of the body. Subcutaneous adipose tissue in humans is less area specific as it is spread as a continuous layer beneath the skin. There are also apparent differences in adipocyte location between sexes as males tend to have more adipose tissue in the abdominal area and females have more developed mammary and gluteofemoral subcutaneous adipose tissue. In average, females also have a slightly higher adipose body percentage than men, 1(4-28% vs. 8-18%) [1].

Adipose tissue can be divided into two main types, white and brown adipose tissue, (WAT and BAT, respectively). They are discussed briefly below.

Brown adipocyte tissue

Brown adipocytes have a multilocular distribution of TG droplets and a vast number of specialized mitochondria which contains the uniquely BAT expressed protein, uncoupling protein-1 (UCP1). The main physiological role of BAT is thermogenesis which is believed to be TG fueled heat production through UCP-1 driven mitochondrial combustion of substrates uncoupled from the production of ATP [2]. In small and young endothermic animals, with high surface to volume body ratio and less heat generation from muscle movement, BAT is more abundant and expresses more UCP-1 than in larger mammals.

White adipocyte tissue

The WAT consists mainly of mature white adipocytes, but stromal vascular cells (including preadipocytes, fibroblasts and macrophages) can constitute up to 50% of the cellular content [3]. Preadipocytes are fibroblast-like cells determined to the adipocyte cell lineage. As mature adipocytes cannot proliferate, these cells function as source for new adipocytes in tissue turnover or expansion [4, 5]. The monocyte derived macrophages mainly remove foreign particles and dead cells in the adipose tissue, as well as initiating the immune response after an infection [6]. Lately the stromal vascular portion of the adipose tissue has been shown to contain cells that are able to undergo adipogenic (fat), osteogenic (bone), chondrogenic (cartilage), and myogenic (muscle) differentiation *in vitro* [7, 8]. Whether this is an indication of the presence of a multipotent stem cell within the tissue or only reflect the presence of several progenitor cells are still unclear.

1.2 Adipocyte function

1.2.1 Lipid metabolism

The main functions of adipocytes are uptake and release of free fatty acids (FFAs) and glucose from the extracellular matrix, lipogenesis (TG synthesis) and lipolysis (TG hydrolysis). Figure 1 gives an overview of the key steps and regulation pathways of these processes. Up to 85% of a white adipocyte consists of TG [3], which usually is located in a unilocular vacuole called a lipid droplet emphasizing the importance of lipid metabolism in the cell.

Hydrolysis of TG in the adipocytes leads to the release of FFA and glycerol into the bloodstream. FFA serves as a source of energy and glycerol is transported to the liver for reuse [9]. The rate limiting step in TG release is the hydrolysis of TG mediated by adipose triglyceride lipase (ATGL) and hormone-sensitive lipase (HSL) that hydrolyze TG and diacylglycerol (DG), respectively. HSL translocates to the TG pool of the cell when phosphorylated directly by protein kinase A (PKA), a cyclic AMP (cAMP) activated kinase. The phospho protein perilipin A also moves to the TG pool

upon phosphorylation by PKA. Here it activates ATGL by a yet uncharacterized mechanism [10]. The rise in cAMP levels leading to PKA activation and hence lipolysis is positively regulated by adenylyl cyclase (AC) and is negatively regulated by phosphodiesterase (PDE). Activation of AC, generating cAMP from ATP, happens through a stimulatory G-protein (G_S) which binds to the adrenergic receptor beta (ARβ). This activation of AC can be countered by an inhibitory G protein (G_I) transmitting a signal from ARα_2. In adipocytes the PDE isoform 3B negatively regulates cAMP leves by converting it to AMP. Tumor necrosis factor alpha (TNFα) negatively regulates both PDE3B expression and activity through its pathway (addressed in 1.4). In addition TNFα inhibits the action of G_I on AC [11]. Insulin inhibits PKA action through PDE3B activation (see below).

After a meal there is a switch in adipocyte biology from release of FFA to uptake and TG synthesis. FFAs are either synthesized *de novo* from glucose or recycled from the cytosol and extracellular fluid. Lipoprotein lipase (LPL) expressed on the surface of endothelial cells in the adipose tissue hydrolyzes circulating TG to FFA. FFA transport into adipocytes is mediated by fatty acid transporter proteins (FATPs). Imported FFAs are chaperoned by adipocyte fatty acid binding protein P2 (aP2) for re-esterfication and conjugation to coenzyme A (coA) catalyzed by acyl CoA synthetases (ACS) [12]. Both *de novo* synthesized FFA and recycled FFA are joined with G3P (3-glycerol phosphate) to produce TG [13]. Adipocytes lack the glycerokinase protein and cannot recycle glycerol for the lipolysis process. Therefore, glucose is the main source of G3P for the adipocyte [14].

Insulin, a hormone secreted from pancreatic β cells, is a key factor in regulation of adipocyte lipid metabolism and glucose uptake. Insulin levels rise in fed state and fall in fasting [15]. Insulin acts mainly through insulin-like growth factor insulin receptor (IGF-IR) and insulin receptor (IR). IGF-IR transduces activation of Ras and protein kinase B (PKB) downstream pathways, while IR mediates signaling on IR substrate 1(IRS-1) subsequently activating phosphatidylinositol-3 kinase (PI-3K) and also PKB [16]. Insulin promotes TG synthesis by initiating translocation of FATP1 and FATP4 and glucose transporter 4 (GLUT4) from intracellular vesicles to the plasma

membrane, increasing the imported FFA and glucose needed for lipogenesis [17]. Insulin also inhibits lipolysis by phosphorylation and activation of PDE3B mediated by PKB [11].

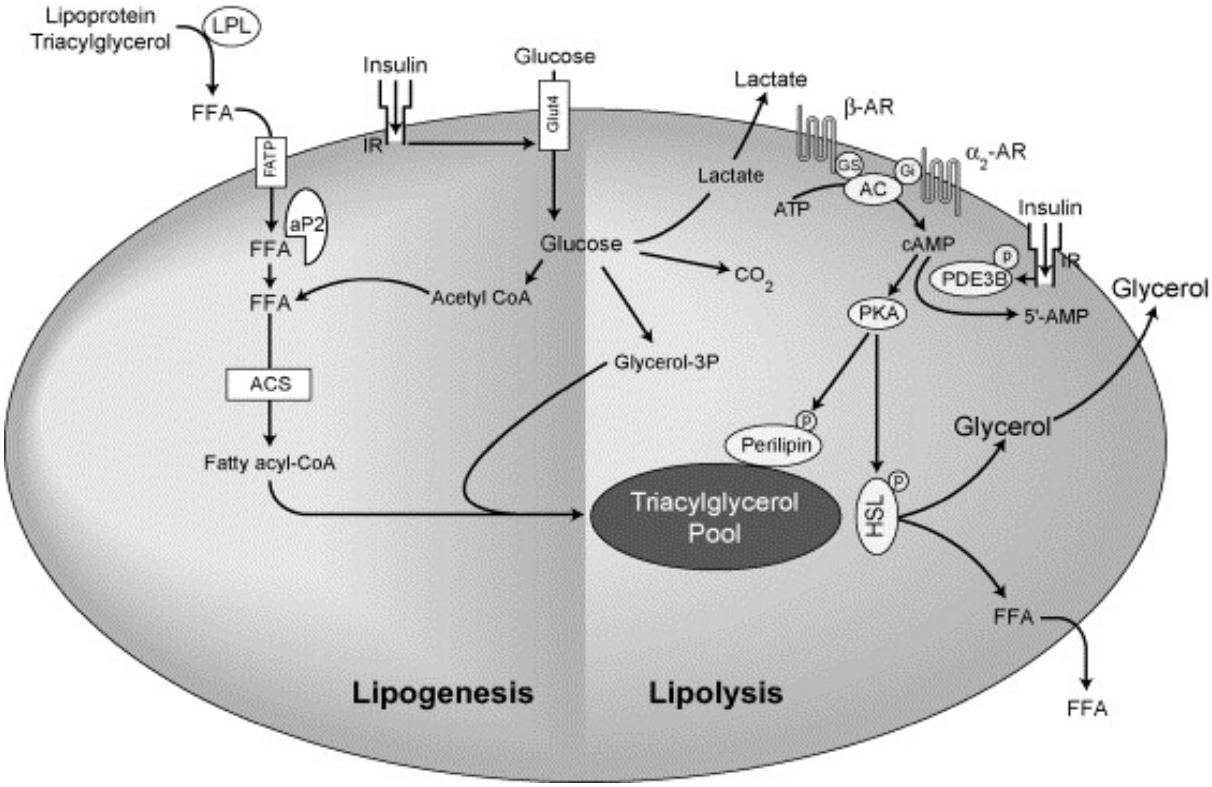

Figure 1. O**verview of the main pathways in adipocyte lipid metabolism**. Reprinted, with permission from "Subcutaneous fat in normal and diseased states" by Avram, Avram et al. in journal for American Academy of Dermatology (2005) [9].

The basics for the fat storage and metabolism in the adipocyte have been known since the 1970s. However, the adipocyte gained much more attention after the surprising discoveries in the 1990s made it clear that white adipocytes also act as an endocrine organ playing a major part in the systemic regulation of energy balance by release of adipocyte specific hormones called adipokines. Below, details about the most common adipokines are discussed.

1.2.2 Endocrine action of the adipocyte

Leptin

The best characterized adipokine was cloned in 1994 and identified as the product of the *ob* gene responsible for genetic obesity in deficient mice (ob/ob mice) [18]. Shortly after it was given the name leptin after "leptos" Greek for thin, as injections of a recombinant form of the protein reversed obesity on ob/ob mice [19]. When secreted from adipocytes and released into the blood leptin acts on many tissues and induces effects on muscles, bones, pancreatic beta cells, immune cells and also several other tissues and organs. However, the most important effect is believed to be on the Central Nervous System (CNS). Leptin is transported across the blood brain barrier (BBB) to reach the CNS and the hypothalamus where it targets two populations of neurons. Activation of neurons promoting energy expenditure and weight loss containing pro-opiomelanocortin (POMC)/cocaine and amphetamine-regulated transcripts and inhibition of different neurons promoting food intake and weight gain expressing neuropeptide Y (NPY)/agouti-related peptide (AgRP), the latter group of neurons being suppressors of the former. Leptin signals through the leptin receptor (OB-Rb) which activates JAK/STAT (Janus kinase/Signal Transducer and Activator of Transcription) signaling among other pathways [13, 20]. Hepatocytes, adipocytes, heart, β cells of the pancreas and immune cells express the OB-Rb. Paracrine effects of leptin have shown importance in regulating oxidation of lipids and preventing ectopic lipid accumulation [21, 22]. Except fat mass, many other factors influence leptin levels: insulin, glucocorticoids, TNFα, estrogens and C/EBPα (CCAAT/Enhancer Binding Protein alfa) all increase leptin expression and secretion; conversely, β3-adrenergic activity, androgens, FFA, growth hormone (GH) and Peroxisome Proliferator-Activated Receptor gamma (PPARγ) agonists leads to decreased leptin levels [23].

Adiponectin

Adiponectin is a protein that belongs to the collagen superfamily. It is uniquely expressed and secreted by mature adipocytes, especially in subcutaneous adipose tissue, and in extremely high concentrations. Adiponectin accounts for ~0.01% of all

serum proteins. In contrast to leptin, adiponectin levels are reduced with obesity and elevated during starvation. Adiponectin impacts body metabolism by increasing insulin sensitivity in metabolic tissues, such as muscle, adipose tissue and liver. In muscles it binds to Adiponectin Receptor 1 (AdipoR1) and promotes glucose uptake and FFA oxidation; in liver it binds AdipoR2, promotes FFA oxidation and decreases gluconeogenesis (the generation of 3-glycerol phosphate from precursors other than glucose) [24]. Downstream signaling of AdipoR1 is not well characterized, but is known to involve activation of p38 mitogen activated protein kinase (MAPK) and PPARα. Aside from metabolic effects, adiponectin executes anti-inflammatory effects through inhibition of NF-κB signaling and induction of several inflammatory cytokines in human monocytes, macrophages and dendritic cells [25, 26].

RBP4

Retinol binding protein 4 (RBP4) is a plasma transport protein for retinol and is up-regulated in adipose tissue in mice deficient in GLUT4. RBP4 is elevated in obese and obese-diabetic human and mice, and overexpression of RBP4 in mice leads to increased insulin resistance [27]. RBP4 secretion by adipose tissue is suggested to be a reponse to low glucose blood levels detected by GLUT4. RBP4 suppresses insulin signals in muscles inhibiting the activity of PI-3K and IRS-1 phosphorylation, while increasing the glucose production in the liver increasing plasma glucose concentration [25, 27].

Visfatin

Visfatin, originally identified as pre-B-cell colony-enhancing factor (PBEF) that is expressed in bone marrow, liver and muscles over a decade ago, has been re-identified in adipose tissue as a factor that is up-regulated during development of obesity. The visceral tissue specificity of visfatin is still controversial, and its supposed role in binding and activation of the insulin receptor need further proof, but its connection to adiposity is still strong [28-30].

PAI-1

Plasminogen Activator Inhibitor-1 (PAI-1) regulates the coagulation cascade as an inhibitor of fibrinolysis and inactivation of urokinase-type and tissue-type plasminogen activator. PAI-1 also has proposed roles in atherogenesis and angiogenesis. PAI-1 is expressed in many cell types within the adipose tissue and its levels correlate with visceral adiposity [23, 31].

MCP-1

Monocyte chemoattractant protein 1 (MCP-1) is involved in recruiting monocytes and T lymphocytes to sites of injury and infection. This chemokine is expressed in multiple cell types including endothelial, skeletal- and smooth muscle cells as well as adipocytes. The target of MCP-1 is chemokine CC motif receptor 2 (CCR2). Expression of MCP-1 rises with obesity in most fat tissue types, especially in visceral fat. In 3T3-L1 cells, insulin, TNFα, GH and IL-6 all induce MCP-1 expression [32, 33].

1.3 Adipose tissue and obesity

During the last three decades the prevalence of obesity in the United States have doubled for adults (from 15.2% to 30.4%) and children (from 6.5% to 15.8%) and tripled for adolescents (from 15.0% to 16.1%)[34]. The same trend is also seen in Norway and the rest of the world [35, 36]. Estimates suggest that worldwide 400 million people are currently obese [37].

Adipocity in humans is measured by the BMI index which is defined by the body mass in kgs divided by the square of height in meters. People with BMI of ≥ 30 are considered obese [37]. Obesity is correlated with insulin resistance, type 2 diabetes and multiple cardiovascular diseases [38, 39]. Besides personal health problems, a population increased in obese individuals will thus face considerable increased costs in health care expenditures [40, 41].

Genetics do contribute to obesity [42], but an individual cannot become obese without having chronically greater energy intake than expenditure. Energy

expenditure includes physical activity, all voluntary movement, basal metabolism, all vital biochemical processes in the body; adaptive thermogenesis, and heat production generated to cope with climate [43]. Greater energy intake without increasing expenditure will increase TG storage in adipocytes which therefore will expand. Depending on net positive energy intake and genetic make-up of the individual the expansion of the fat tissue in extreme cases of obesity can reach 60 to 70% of total body mass in contrast to the normal 20%. This expansion is governed by enlargement of existing adipocytes (hypertrophy) and differentiation of preadipocytes into adipocytes (hyperplasia) [1, 42].

The exact processes causing the health risks associated with increased fat tissue is still somewhat unclear. Dys-regulation in adipose metabolism and an interaction between the immune system and adipose tissue seem to stand central in this regard. Leptin levels rise with adiposity to promote energy expenditure and prevent plasma lipid accumulation. The effects of leptin, however, diminish with higher levels as tissues affected by leptin through its OB-Rb, develop resistance. The resistance is thought to be mediated in two ways: leptin action on the CNS is lost by impaired transport across the BBB, and the general OB-Rb signaling is inhibited by suppressor of cytokine signaling 3 (SOCS3) that acts as an intracellular negative feedback pathway from JAK/STAT activation [20, 21]. SOCS3, however, also inhibits IRS-1, a downstream signal of insulin action, hence leptin can contribute to insulin resistance [44]. In addition, leptin acts as a pro-inflammatory signal on the innate and adaptive immune system and in that way be a possible mediator of increased immune reaction to obesity [31].

Both hypertrophy of the adipocyte and increasing levels of cytokines (addressed below) contribute to the increased lipolysis and stunted TG synthesis in the adipose tissue that is linked to obesity. The elevated plasma levels of FFAs are thought to have an especially important role in whole body insulin resistance as it inhibits insulin signaling, glucose uptake and glucagon synthesis in the muscles, and promotes glucose production in the liver [45, 46].

Two factors secreted by adipose tissue, TNFα and IL-6 (Interleukin 6), are both important pro-inflammatory cytokines [26]. Adipose tissue contributes up to a third of the circulating levels of IL-6. But considering its levels within the adipose tissue, which are 100 times higher than the circulation, IL-6 para- and autocrine functions have been more studied. During obesity IL-6 levels rise. Importantly, non-fat cells are the main secretors [47]. IL-6 promotes insulin resistance by inducing SOCS3 and lipolysis and by inhibition of adipogenesis and adiponectin secretion [47, 48]. IL-6 have also been suggested to have a role in the early stages of arteriosclerosis [49]. The increasing levels of TNFα correlated to obesity are mainly secreted by macrophages accumulating in adipose tissue [49]. Indeed, in lean individuals macrophages contribute to 5-10% of the total cells in adipose tissue while in obesity this can increase up to 50% [50]. TNFα binds to the TNF receptor and activates the c-Jun N-terminal kinase (JNK) pathway and/or nuclear factor κB (NFκB) through activation of inhibitor of NF-κB (IκB) kinase (IKKβ). Increased JNK activity in obesity leads to fortified insulin resistance as IRS-1 activity is decreased [51]. TNFα affects the expression of several adipokines with central roles in mediating the health risks associated with obesity; adiponectin levels decrease, leptin increase, more FFAs are released, circulating PAI-1 levels are elevated, and more MCP-1 is secreted [23, 32, 49].

A major factor promoting the macrophage migration to the adipose tissue during increased obesity is MCP-1. In addition to the factors leading to increased MCP-1 secretion mentioned above, hypertrophied adipocytes release more MCP-1 [52]. Other than the role in mediating a low grade chronic inflammation of the adipose tissue [44], MCP-1 increase insulin resistance and its elevated plasma levels are linked to development of atherosclerosis [50].

Hyperplasia and hypertrophy are necessary for the adipose expansion [1]. Since mature adipocytes do not undergo mitotic expansion [53], understanding the mechanisms of adipocyte development from precursor cells are important and may provide clues as to how to manage the increasing obesity epidemic.

1.4 Adipose development

Adipocytes are considered to derive from the mesoderm germ layer, although questions have been raised whether mesodermal tissue is the only possible origin for adipocytes [42, 54]. The mesenchymal stem cells (MSCs) were first identified in human bone marrow and are used as a cell model for mesoderm tissue [42]. Both *in vitro* and *in vivo* studies have found MSCs to be capable of differentiating into a range of cell types including chondrocytes, adipocytes, myocytes, cardiomyocytes and bone marrow stromal cells [55]. The steps in differentiation of MSCs have been less characterized as they are indistinguishable from fibroblasts morphologically, and although some cell markers that can distinguish MSCs from other cells have been identified, no markers for distinct steps during early development have been found [56]. There has been some success in determining factors and pathways affecting the early development of MSCs. In the differentiation program towards the adipocyte lineage stimulation by bone morphogenic protein 2 and 4 (BMP2/4) can commit multipotent cells to adipocyte lineage and/or augment their adipocyte differentiation, through both Small mothers against decapentaplegic (Smad)- and p38-dependent mechanisms [57]. Tumor growth factor beta (TGF-β) inhibits adipocyte differentiation by inactivating C/EBP transcription factors via physical interaction with Smad3 [58]. In addition transcription factor activation through Wnt signaling have been found activate the early events of adipogenesis [59].

The mouse preadipocyte cell-lines 3T3-L1 F422A and 3T3-L1 have been widely used as model systems to study adipogenesis. These cells have the morphology of fibroblasts, but are committed to the adipocyte lineage [42, 60]. Below sections review the key steps in the differentiation of 3T3-L1 cells to a mature adipocyte.

1.4.1 Adipogenesis

Differentiation of a preadipocyte into a mature adipocyte is commonly divided into 3 stages: growth arrest, mitotic clonal expansion (MCE), and terminal differentiation [61] (depicted in Figure 2). Growth arrest of the preadipocytes (in G_0/G_i phase) occurs by contact-inhibition. At this point addition of prodifferentiative hormones will signal the arrested preadipocytes to re-enter the cell cycle and undergo several rounds of cell division, known as the MCE. There has been some controversy whether the MCE is required for differentiation [61]. Following the MCE, preadipocytes enter a unique growth arrested stage, G_D (D for differentiation), considered to be a poorly defined point of no return for commitment to terminal differentiation. During terminal differentiation 3T3-L1 cells transform from their fibroblastic morphology into the appearance associated with mature adipocytes, with a round shape and lipid filled vacuoles, as well as with their biochemical characteristics [53].

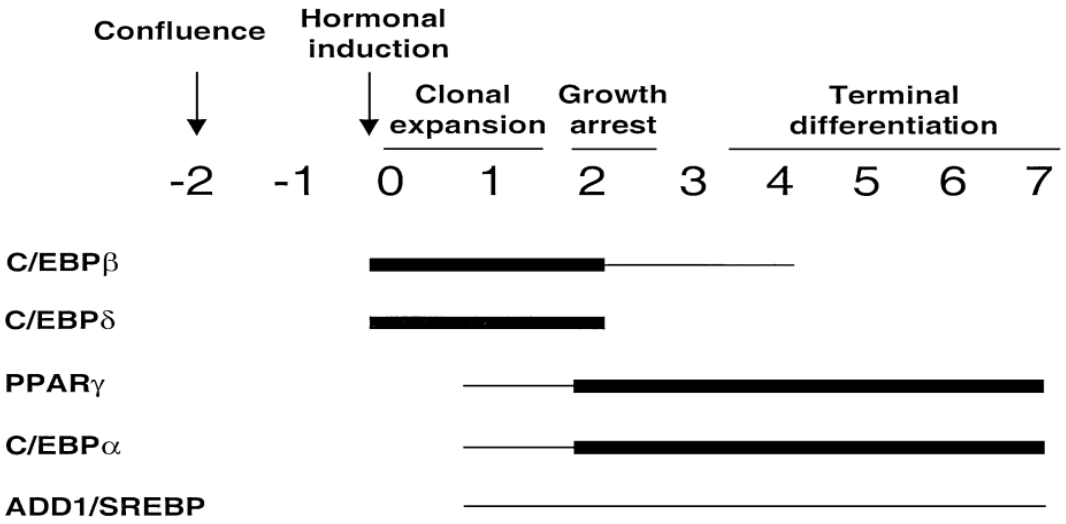

Figure 2. **Temporal expression of the major transcription factors involved in differentiation of preadipocytic cell lines**. See the text for more details. Thick line, higher expression level; thin line, lower expression level. Reprinted, with permission, from the Annual Review of Nutrition, Volume 20 ©2000 by Annual Reviews www.annualreviews.org [62].

Below is a review of the most important transcription factors (TFs) that have a role in differentiation of preadipocytes.

1.4.2 PPARγ

The Peroxisome Proliferator-Activated Receptor (PPAR) belongs to a family with three members, α, δ and γ forms, and is member of the nuclear hormone receptor (NHR) superfamily. PPARs heterodimerize with the retinoid X receptor (RXR) prior to DNA binding [63]. From the PPAR family, it is PPARγ which is relevant for adipogenesis [64]. Multiple FFAs and their derivates, as well as certain eicosanoids (e.g. the prostaglandin J_2), act as low affinity ligands for PPARγ, but an endogenous PPARγ ligand has not been identified. Nevertheless, several synthetic agonists are available, e.g. the thiazolidinediones (TZD) which are used in the clinic as insulin sensitizers [64]. PPARγ is responsible for activating many, if not most, of the genes involved in adipose tissue associated processes: fatty acid binding, storage and metabolism, and gluconeogenesis; e.g. aP2, LPL and acyl-CoA oxidase (ACO), which catalyze the first step in fatty acid β oxidation [65]. Three isoforms of PPARγ have been identified, $\gamma_{1\text{-}3}$, γ_1 and γ_3 code for the same protein product but from different transcripts and are ubiquitously expressed while PPARγ_2 is unique to the adipose tissue. The specific role of the different isoforms during adipogenesis is still unclear [61, 66]. The important role of PPARγ in adipocyte differentiation has been demonstrated through multiple experiments including *in vitro* overexpression and knockdown, as well as *in vivo* gene targeting in mice [67-71]. Knowledge drawn from these experiments, emphasize PPARγ as necessary and sufficient for adipogenesis.

1.4.3 C/EBP family

C/EBPs (CCAAT/Enhancer Binding Protein) is a family of six (α, β, γ, δ, ε and ζ) highly conserved transcription factors, containing a leucine zipper domain involved in dimerization and DNA binding. In adipocytes, three members of the family are implicated as positive regulators of adipogenesis; C/EBPα, C/EBPβ, and C/EBPδ [72]. C/EBPα acts as a promoter for many adipocyte genes such as GLUT4, leptin and aP2 [73]. Studies in fibroblasts lacking PPARγ found that C/EBPα alone is unable to induce differentiation, suggesting that C/EBPα and PPARγ participate in

the same pathway [74]. C/EBPα has been linked to different features of adipogenesis, such as growth arrest, insulin sensitivity and promoting the expression of PPARγ and own gene through differentiation [75-78].

C/EBPβ and C/EBPδ are expressed early after induction of adipogenesis [79]. Ectopic expression of C/EBPβ, but not C/EBPδ alone, has proven to be sufficient to induce differentiation in vitro [79-81]. In defining the order of actions towards terminal differentiation recent studies have shown that C/EBPβ, but not C/EBPα, induces PPARγ expression in the absence of PPARγ or PPARγ ligand. This leads to a model showing early induction of C/EBPβ and C/EBPδ after induction of differentiation, which activate expression of PPARγ. PPARγ, possibly concert with C/EBPβ and C/EBPδ, then facilitates C/EBPα expression [82]. C/EBPβ is induced by cAMP levels through CREB [83]. DNA binding of C/EBPβ at the centromeres seems to be pre-required for initiation of MCE [84, 85].

Two other members of the C/EBP family, CHOP-10(C/EBPζ) and C/EBPγ, have been suggested as inhibitors of adipogenesis. They heterodimerize with C/EBPβ causing its inactivation and disrupt its DNA binding [73].

1.4.4 KLF

Another group of transcription factors regulating adipogenesis is KLF (Krüppel Like Factors). Several members of this large C2H2-zinc finger family play a role during adipocyte differentiation. KLF2 binds the promoter of PPARγ_2 and represses its activation, thereby inhibiting adipogenesis [66, 86]. After induction of differentiation, expressed KLF5, induced by C/EBPβ and C/EBPδ, dispatch KLF2. This promotes PPARγ_2 expression. Later in development KLF5 is downregulated and expression of the proadipogenic KLF15 increases. KLF15 also promotes PPARγ_2 expression in addition to promoting expression of genes associated with mature adipocytes (e.g. GLUt4) [87]. Other KLFs that have been shown to act in adipogenesis are KLF7, KLF6, KLF3 and KLF4. KLF4 has been shown to be induced in response to cAMP and in cooperation with KROX20, which is a proadipogenic factor [88], that promotes expression of C/EBPβ [66, 89, 90].

1.4.5 Other factors invoved in adipogenesis

ADD1/SREBP-1c belongs to a transcription factor family known to regulate genes important in cholesterol and fatty acid metabolism, SREBP (Sterol Regulatory Element Binding Protein). ADD1/SREBP-1c is expressed early after induction of adipogenesis and activated by insulin action [91]. Expression studies have indicated that ADD1/SREBP-1c promotes secretion and/or synthesis of natural ligand for PPARγ independent of the C/EBPβ pathway [92, 93].

The E2F (adenovirus E2 promoter binding factor) transcription factor family is essential in regulating the cell cycle. E2Fs seem to play their main function in the transition from growth arrested preadipocytes into the MCE as free E2F/DP heterodimers or in complexes with pocket family proteins (pRB, p107, p130) and cyclin/cdk protein family members. E2F4 and 5 act as repressors, and when active, prevent progression into MCE. E2F1-3 act as activators and E2F1 induces PPARγ transcription during MCE [94].

The zinc finger transcription family GATA has its name from the consensus sequence which they recognize. Out of the 6 GATA proteins, GATA2 and GATA3 are expressed in adipocytes [95]. These inhibit adipogenesis by interacting with C/EBPα and β as well as suppressing expression of PPARγ by acting on its promoter [96].

FoxA2 and FoxO1, members of the forkhead box protein family, are both thought to have inhibitory effects on adipocyte development prior to and in the early stages of differentiation. FoxA2 inhibits adipogenesis by preventing the downregulation of Pref-1, Gata-2, and Gata-3 (Pref-1 being a marker for preadipocytes and anti-adipogenic factor) [97, 98], and FoxO1 by preventing MCE as its associated with increased expression of cell cycle inhibitors [99].

STAT (Signal Transducers and Activators of Transcription) are a family of seven members (STAT1-4, 5A, 5B, 6). STATs are activated through tyrosine phosphorylation by Janus kinases (JAKs) that respond to signals form a family of cytokine receptors that are activated by a range of growth factors, hormones and

cytokines. During differentiation in 3T3-L1 cells, expression of STAT1, STAT3 and STAT5 has been observed. The mechanisms of STATs action on adipogenesis is still unclear [100]. Recent studies have pointed out STAT3 as an anti-adipogenic factor [101], and STAT5, in particular STAT5A, as a pro-adipogenic factor [102, 103].

Extracellular signals exert their effects either by a direct impact on transcription factor expression levels or by affecting their activity, e.g. through co-factor recruitment and/or modification. One widely used modification in the cell in response to extracellular ques is phosphorylation through kinase pathways. A major kinase pathway in the cell, MAPKs, has a role in adipogenesis and is further discussed below.

1.5 MAPK signaling pathway

1.5.1 General structure and function

The mitogen activated protein kinases (MAPKs) are ubiquitously expressed, highly conserved serine/threonine kinases and involved in pathways controlling embryogenesis, cell differentiation, cell proliferation and cell death [104, 105]. In mammals 14 MAPK genes identified to date have been grouped in 7 distinct families based on a motif in their activation loop and activation pathway: extracellular signal-regulated kinase 1/2 (ERK1/2), c-Jun N-terminal kinase 1-3(JNK1-3), p38 (α, β, γ, δ), ERK5, ERK3/4, Nemo-like kinase (NLK) and ERK7, the four former being considered the main families and will be the ones referred to from now on [105-107]. The three MAPK families share a threonine-X-tyrosine motif within their active loop. Both the threonine and tyrosine residues need to be phosphorylated to activate the MAPK. Highly specific MAPK kinases (MAP2Ks) phosphorylate the MAPKs. The MAP2Ks are under activational control by MAP2K kinases (MAP3Ks), giving a three step phosphorylation cascade transducing signals from numerous stimuli, including growth factors, mitogens, inflammatory cytokines and cellular stress. Activated MAPK phosphorylates cytosolic targets and translocates into the nucleus to execute its actions on gene expression. The final actions of the MAPKs depend on

several features of the phosphorylation cascade. Amplification of the signal can be achieved when the substrate kinase is more abundant than the activated kinase. Furthermore, with overlapping substrate specificity among the MAPKs the pathways have integrated responses. Another interesting future of the MAPK cascade is the scaffold proteins and docking motifs on the MAPKs which assure fast and accurate signal transfer and are also target of pathway regulation [105].

Figure 3 gives a simplified overview of the different pathways of the MAPK cascades and their functions. The cellular responses to the MAPK are in large part mediated by downstream phosphorylation of a variety of transcription factors, for reviews, see [105, 108].

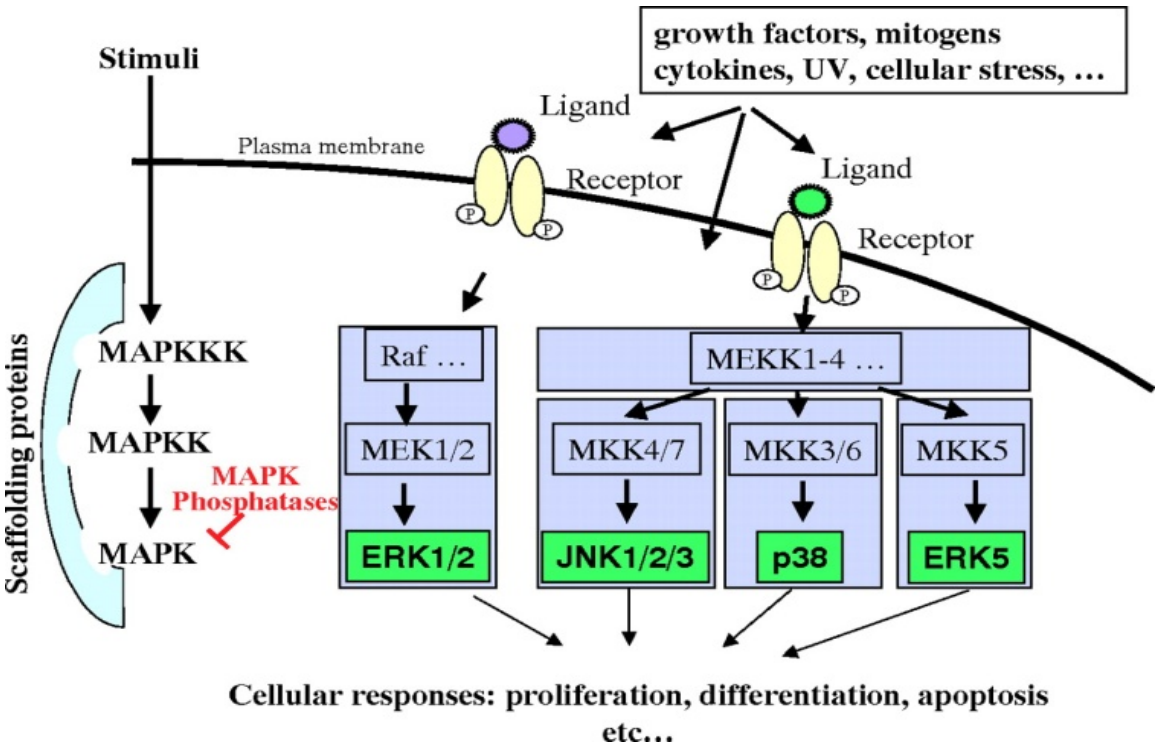

Figure 3. **A schematic overview of the main MAPK family pathways**. For details see text below. Reprinted, with permission from "Concise review: regulation of embryonic stem cell lineage commitment by mitogen-activated protein kinases" by Binetruy, Heasley et al. Stem Cells (2007) [109].

The ERK pathway is mainly associated with promoting cell growth, cell proliferation and cell survival in response to mitogens and growth factors. Ras, a small GTPase, transmits most extracellular signals through activation of the Raf MAP3K family. The Rafs subsequentially phosphorylate MEK1/2, the upstream activators of ERK,

that in turn phosphorylate ERK at the threonine-glutamate-tyrosine motif which results in ERK activation [105, 110].

JNK, also called the stress activated MAPK (SAPK), is activated by phosphorylation of the Threonine-Proline-Tyrosine motif and mediates response to various stress stimuli (e.g. UV-light, heat, osmotic shock), inflammatory cytokines (IL-6, TNFα) and growth factors. MKK4 and MKK7 are the upstream MAP2Ks for JNK. MKK7 mainly mediates cell responses to cytokines while MKK4 is activated by stress; in addition to JNK, MKK4 also activates p38. Furthermore, MKK4 and MKK7 seem to preferentially phosphorylate JNK on tyrosine and threonine, respectively, indicating cooperative activation [111]. MKK4 and MKK7 activation is induced by a number of different MAP3Ks, many shared with the p38 pathway [112]. In addition to influencing the inflammatory response, metabolism and cell transformation through activation of various transcription factors, JNK plays an important role in apoptosis/cell survival by inhibiting the antiapoptotic proteins Bcl-2 and Bcl-xl [111, 113].

The pathway of p38 activation is highly integrated with the pathway of JNK and responds to similar stimuli. MKK3 and 6 are specific activators of p38 while MKK4 is shared with JNK. They all activate p38 by phosphorylating the threonine-glycine-tyrosine motif. As mentioned above JNK and p38 share most of the same MAP3K. p21 activated kinases (PAKs), however, seem to be exclusive for p38. Upstream of the MAP3K GTPases of the Rho family contribute to p38 activation. The downstream effects display great variety including inflammation, cell cycle regulation, cell death, senescence and tumorgenesis. These responses, however, seem to be specific with regard to cell type [107].

ERK5, also known as big MAPK1 (BMKP1), shares activation motif with ERK but differs from it and the other two MAPKs as it is considerably larger (~88 kDa vs. 38-54 kDa). Although sharing activation signal with all the other MAPKs, ERK5 displays a narrow pathway specificity, being specifically phosphorylated by only the

MAP2K MKK5. Of the MAP3Ks, the MEKK family are the main transducers of signals [108].

1.5.2 MAPKs in adipogenesis

ERK pathway was linked to adipogenesis in 1991 when it was shown that ectopic expression of an active Ras mutant led to growth arrest and terminal differentiation of 3T3-L1 cells in the absence of insulin and IGF-1 [114]. Later inhibition of ERK expression was found to suppress adipogenesis [115]. However, in response to various growth factors, ERK has been shown to inhibit PPARγ activity by direct phosphorylation thereby suppressing adipogenesis [116, 117]. The seemingly incompatible findings that ERK could both induce and inhibit adipogenesis were put in context with a model for temporal regulation of ERK. The ERK pathway was found to be necessary for the MCE that is prior to terminal differentiation [118]. Another study showed ERK to be activated immediately after induction of differentiation inducing expression of transcription factors central in adipogenesis (C/EBPα and PPARγ), followed by a rapid inactivation [119]. Later the effect of ERK on C/EBPα and PPARγ expression has been linked to an activational phosphorylation of C/EBPβ [120]. In vivo studies with ERK1-/- knockout mice have indicated that ERK1 but not ERK2, is the isoform active in adipogenesis [121]. ERK1-/- mice are protected from insulin resistance and high fat diet induced obesity supporting the *in vitro* findings [122].

As ERK, p38 and JNK show an induced activation immediately after induction of adipogenesis in 3T3-L1 cells [123]. Studies done with p38 inhibitors in 3T3-L1 cells have linked p38 activation to phosphorylation of C/EBPβ leading to its activation, as seen with ERK, and subsequent promotion of adipogenesis [124, 125]. Further evidence for p38 acting in a proadipogenic manner was shown by overexpression of active MKK6 [126]. This dominant active mutant was sufficient to induce activation without any hormonal stimulation. However, prolonged overexpression induced massive cell death. Two additional reports further support p38 as an enhancer of adipocyte development [127, 128]. In opposition to these results p38 has been found

to activate CHOP leading to inhibition of C/EBPβ [129, 130]. In addition, a study of p38 action in adipocyte development using multiple cell lines found that its knockdown and inhibition promoted adipogenesis. The authors suggested that cell line differences was the cause of variation [131].

Few roles have been pinned to JNK in adipogenesis, although JNK activation have shown to inhibit PPARγ [132]. JNK1 and JIP1 (JNK interacting protein 1) have been suggested a role in development of obesity, as deficiency of JIP1 mice and absence of JNK1 in ob/ob mice was linked to resistance to obesity [133, 134].

There is currently limited information on the possible role of ERK5 in adipogenesis. A recent study, have proposed a small role for ERK5 overlapping with the action of ERK in adipogenesis [135].

1.6 MAPK Phosphatases

1.6.1 General features

The dual specificity phosphatases (DUSPs) also known as MAPK Phosphatases (MKPs) consist of a subfamily of the superfamily of protein tyrosine phosphatases (PTP) that can dephosphorylate both phospho-tyrosine and phospho-threonine. It is common to separate the MKPs in a group of typical MKPs and atypical MKPs, with 11 and 19 family members, respectively [136]. All typical MKPs, except a catalytically inactive (DUSP24), regulate MAPK activity through dephosphorylation of the TXY-motif (Table 1). Several atypical MKPs have also been shown to have MAPK as substrate, discussed below [137].

DUSPs have a catalytic dual specific phosphatase (DSP) domain at the C-terminus with the conserved motif HCXXXXXR (Histidine, Cysteine, X is any amino acid and Arginine) [138]. The DSP motif has no strict preference for any of the MAPKs, so typical MKPs have a MAPK binding (MKB) motif at the N-terminal end. This motif regulates specificity, but in the case of some MKPs also the activity as binding with the MKB motif induces catalytic activity by a conformation change [139].

The classification of MKPs has been done with emphasis on DNA or amino acid sequence similarity, protein structure, substrate specificity and/or subcellular localization resulting in differences in classifying the MKPs [138, 140, 141]. Table 1 summarizes features of the typical MKPs, such as substrate specificity and subcellular localization.

Gene/MKP	Trivial names	Chromosomal localization	Subcellular localization	Substrate specificity	Physiological function(s)
DUSP1/ MKP1	CL100, erp, 3CH134, hVH1	5q34	Nuclear	JNK, p38, ERK	Negative regulator of immune function. Protects mice from lethal endotoxic shock. Plays a key role in metabolic homeostasis and mediates resistance to cellular stress in mouse fibroblasts
DUSP4/ MKP2	Typ1, Sty8, hVH2	8p12-p11	Nuclear	JNK, p38, ERK	Unknown
DUSP2/ None	PAC-1	2q11	Nuclear	ERK, p38	Positive regulator of inflammatory responses. Knockout mice are resistant to immune inflammation
DUSP5/ None	hVH-3, B23	10q25	Nuclear	ERK	Unknown
DUSP6/ MKP3	Pyst1, rVH6	12q22-q23	Cytoplasmic	ERK	Negative feedback regulator of ERK2 downstream of FGFR signaling
DUSP7/ MKP-X	Pyst2, B59	3p21	Cytoplasmic	ERK	Unknown
DUSP9/ MKP4	Pyst3	Xq28	Cytoplasmic	ERK>p38	Essential for placental development and function (labyrinth formation)
DUSP8/ None	M3/6, hVH5, HB5	11p15.5	Cytoplasmic/ nuclear	JNK, p38	Unknown
DUSP10/ MKP5		1q41	Cytoplasmic/ nuclear	JNK, p38	Functions in innate and adaptive immunity
DUSP16/ MKP7		12p12	Cytoplasmic/ nuclear	JNK, p38	Unknown

Table 1. **Nomenclature, properties and physiological functions of dual-specificity MKPs**. Reprinted, with permission from "Dual-specificity MAP kinase phosphatases (MKPs) and cancer" SM Keyse, Cancer Metastasis Review (2008) [142].

Group I

Members: DUSP1/MKP1, DUSP4/MKP2, DUSP2 and DUSP5. The MKPs of this group consist of 300 to 400 amino acid residues. A nuclear localization signal (NLS)

guides these MKPs to the nucleus where they are induced by many of the same stimuli as the MAPKs. Thus, they are suggested to be involved in negative feedback control of MAPK signaling [139]. The role of MKP1 is best characterized in regulation of immune function [143]. MKP1 deficient macrophages are sensitized in their response to bacterial lipopolysaccharides (LPS) through prolonged and elevated p38 and JNK activities, and display an increase in cytokine production [144, 145]. MKP1 also plays a role in the metabolic homeostasis, addressed below.

Group II

Members: DUSP6/MKP3, DUSP7/MKPX and DUSP9/MKP4. These MKPs have nuclear export signals (NES) and localize to the cytosol. These ~400 amino acid large MKPs display a preference for ERK dephosphorylation [141]. This group has especially been linked to early development. MKP4 knockouts in mice are embryonic lethal as the placenta fail to develop properly [146]. MKP3 is activated by fibroblast growth factor (FGF). Dys-regulation of MKP3 in mice gives a range of developmental issues (e.g. postnatal lethality, skeletal dwarfism and hearing loss) [147, 148].

Group III

Members: DUSP8/VH5, DUSP16/MKP7 and DUSP10/MKP5. These MKPs form a group of larger phosphatases, with VH5 and MKP7 ~650 amino acids and MKP5 almost 500 amino acids [139]. They also have selectivity for p38 and JNK phosphorylation. VH5 and MKP7 have a domain rich in prolines, glutamates, serines and threonines (PEST), suggested to be involved in rapid turnover of the proteins [138, 149]. MKP5 have an identified function in the innate immune system. Macrophages lacking MKP5 show elevated JNK response to LPS stimulation. The elevated JNK activity leads to higher production of cytokines [150]. VH5 has been found to be expressed mainly in the adult brain, heart, and skeletal muscle [151-153].

Atypical MKPs

Five of the atypical MKPs have been found to dephosphorylate MAPKs: DUSP3/VHR, DUSP14/MKP6, DUSP18, DUPS22/VHX and DUSP26/MKP8. Of

these ~200 amino acid short MKPs VHR (*Vaccinia* H1-related) and MKP6 are the most studied [139]. VHR was the first DUSP identified in mammals [154]. In T cells it has been found to negatively regulate ERK and JNK activation [155]. The expression of VHR is not acutely induced, but VHR activity regulation has been found to be dependent on activators. Two have been identified: VRK3 and Zap-70 [156, 157]. Recently VHR has been reported to play an important role in the regulation of cell cycle, as knockdown of VHR leads to cell arrest in G_1/S and G_2/M phase [158]. MKP6 have been suggested to act in a negative feedback loop on T cell CD28 co-stimulatory signal [159].

1.6.2 MKPs in adipogenesis

To date, only two MKPs have been reported to affect adipogenesis and adipocyte function, MKP1 and MKP4 [160, 161]. The effect of MKP1 on adipogenesis was tested with both 3T3-L1 and 3T3-F224A cells. It was found that altering the immediate, but usually transient, expression of MKP1 was associated with induction of differentiation [162-164], This indicates a role for MKP1 in regulating the essential down-regulation of ERK activity during adipogenesis [161]. MKP1 knockout mice display resistance to diet induced obesity. The resistance was proposed to be an effect of lack of only MKP1 nuclear action and not cytosolic action as MAPK action in the cytosol seemed similar in wild type and knockout mice [165]. MKP4 has been found to block insulins negative control of the promoter of PECK (phosphoenol pyruvate carboxykinase) gene [166]. PECK is an important enzyme in glyconeogenesis. Further investigations of the same group showed that MKP4 was present in murine adipocytes and upregulated in ob/ob mice. In addition they found ectopically expressed MKP4 to inhibit adipogenesis and glucose uptake in 3T3-L1 cells. In a very recent publication, MKP1 and MKP4 were indicated induced by dexamethasone in 3T3-L1 cells, and a concominant block of p38 was followed by a reduction in insulin-induced glucose uptake [160]. This suggests a role for MKP1 and MKP4 in insulin resistance.

2. Aim of the project

ERK, p38 and JNK have active kinase activity during adipogenesis and important functional roles of ERK and p38 have been described [119, 123, 131]. Despite this information, the expression profiles of MKPs and whether they have a role in adipogenesis is poorly understood [160, 161, 165]. One exception to this is that MKP1 has been linked to regulation of ERK dependent MCP-1 secretion in hypertrophied 3T3-L1 cells [167].

Previous work in our group (FS lab; Figure 5 and unpublished data) has found that mRNA levels of several MKPs are regulated during adipogenesis in 3T3-L1 cells. Three MKPs with interesting regulation profile from this analysis (VHR, MKP6, and VH5) were chosen for further study.

The goals of this study were to:

- Investigate if the mRNA regulation of VHR is also at the protein level.
- Establish a stable 3T3-L1 cell line expressing MKPs under the control of a tetracycline induced promoter
- Further characterize functional roles of MKPs in adipogenesis.

3. Materials and Methods

3.1.1 Cell culture

3T3-L1, COS-7 and BOSC cells (all ATCC) were cultured in standard medium [DMEM (Lonza) supplemented with standard 10% fetal bovine serum (FBS, PAA), 50U/mL penicillin and 50µg/mL streptomycin (Cambrex), and 2mM L-Glutamine (Cambrex)]. The cells were kept at 37°C in a humidified 5% CO_2, 95% air incubator (Forma Scientific). 60-80% confluent cells were passed in a 1:3/1:4 ratio. 3T3-L1 cells stably expressing TETON were kept in standard medium with 500µg/mL Geneticin/G418 sulphate (Gibco). 3T3-L1 cells stably expressing TETON and TRE-TIGHT His-VHR were kept in standard medium with 500µg/mL G418 and 150µg/mL Hygromycin (Invitrogen). Tetracycline (Tc) depleted medium used with the TETON system, was standard medium supplemented with TET System Approved FBS (Clontech) instead of standard FBS. When using Tc depleted medium it replaced standard medium from the last passage before the start of the experiment. 1µg/mL doxycycline (dox, Sigma) was added to the media to induce expression of the TETON system.

Differentiation of 3T3-L1 cells were induced two days after reached confluency. Cells were treated with a standard induction medium containing fresh serum, 1µM dexamethasone (Sigma), 0.5mM isobutylmethylxanthine (IBMX, Sigma) and 5µg/mL insulin (Sigma)]. After 48 hours the medium was changed to standard medium containing 5µg/mL insulin.

3.1.2 Oil Red O staining

3T3-L1 cells were fixed with 0.5% gluteralaldehyd (EMS) in phosphate buffered saline (PBS), stained with Oil Red O solution [0.15% Oil Red O (Sigma) in 60% isopropanol (Arcus)] for 10-30 minutes (until precipitate was starting to form) and washed before picture was taken with camera (Nikon Coolpix 4500) directly (1X) or through microscope at 200X magnification (Nikon Elipse TS100).

3.1.3 Construction of expression plasmids

The VH5 open reading frame was amplified from a pYX-Asc vector containing the VH5 cDNA (NM_008748) (ATCC) using AccuPrime Pfx DNA Polymerase (Invitrogen) with a standard PCR machine (PTC-200, MJ Research). The PCR program used was as follows: Enzyme activation/DNA denature step 95°C for 2 minutes followed by 20 cycles: denaturing (95°C for 15 seconds), annealing (60°C for 30 seconds), extending (68°C for 2 minutes). The amplified PCR product was run on a 1% agarose gel to verify right size and extracted with QIAquick gel extraction kit (Qiagen). PCR product was cloned into pcDNA4/HISMAX TOPO vector (Invitrogen) and transformed into One Shot TOP10 chemical competent *E.coli* (Invitrogen). Ampicillin selected positive colonies were screened for VH5 insert using whole cell PCR and then sequenced. Mutation-free plasmid was isolated by MIDI prep (GENOMED). Figure 4A displays a vector map of pcDNA4/HISMAX VH5.

The VH5 coding sequence was an amplified form of pcDNA4/HISMAX VH5 with primers that included the His-tag at 5´ sense end and a primer with overhang adding HindIII restriction site at 3´sens end. Amplification and isolation were done and the PCR-product was cloned into pcDNA4/HISMAX TOPO vector, followed by transformation, screening and sequencing as described above. From the new vector pcDNA4/HISMAX His-VH5 a segment containing a His-tag followed by the VH5 coding sequence could be cut out using HindIII (NEB) restriction enzyme. The segment was ligated into the multiple cloning site (MCS) of HindIII cut pREVTRE-TIGHT using T4 ligase (NEB) according to manufacturer`s instructions. Ligated vector was transformed into electro-competent DH10B *E.coli* and screened by restriction enzyme analysis. A positive clone was sequenced and confirmed to be mutation free. Figure 4B display vector map of pREVTRE-TIGHT His-VH5.

All sequencings were performed by the in-house ABI lab core facility (Dept. Molecular Biosciences, University of Oslo, Norway). Sequence analyses were

performed with Sequence Scanner (Applied Biosystems) software for raw data analyses and Vector NTI Advanced 10 (Invitrogen) for alignment analyses.

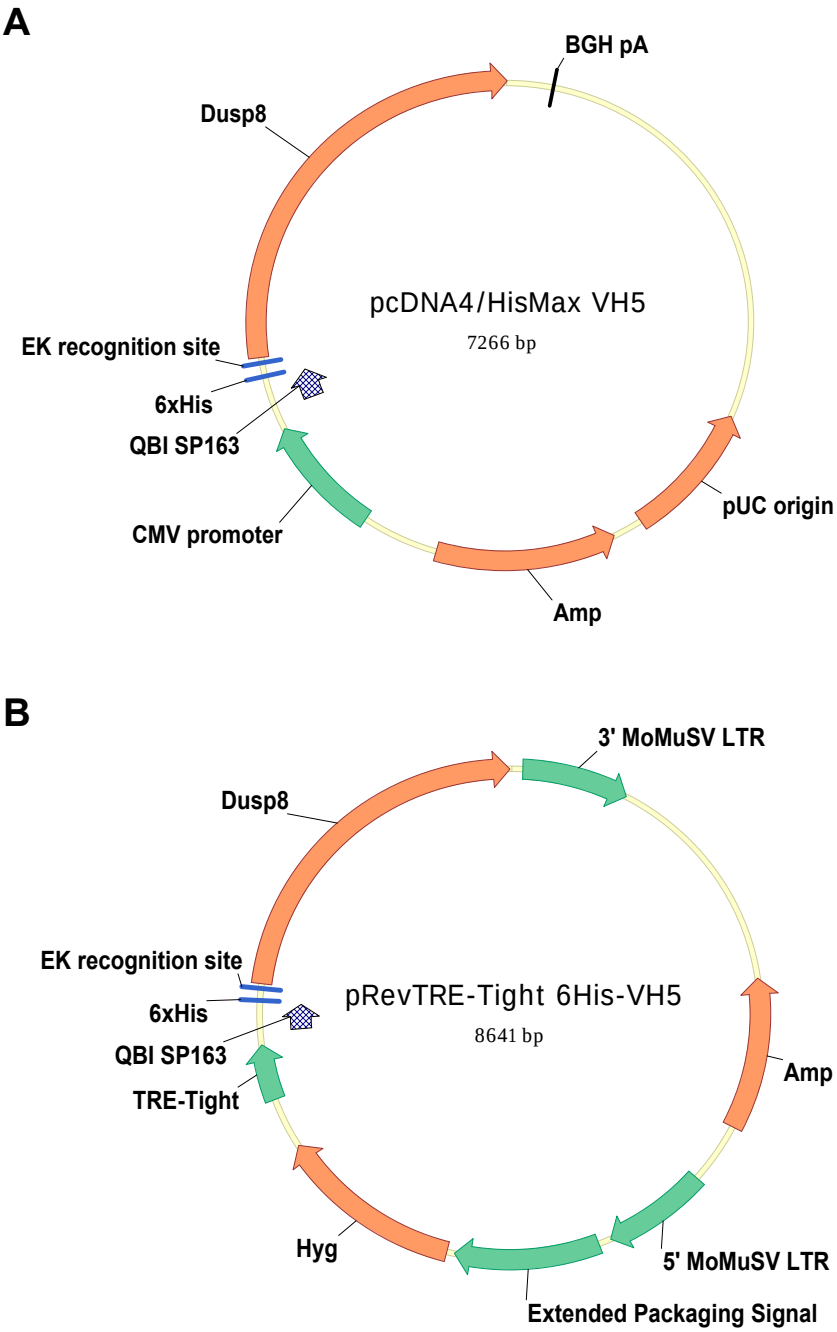

Figure 4. **The VH5 vector constructs**. **A**: Vector product obtained from cloning the VH5 coding sequence into the pcDNA4/HISMAX TOPO vector. **B**: Vector product obtained from cloning the His-VH5 sequence from pcDNA4/HISMAX His-VH5 into pREVTRE-TIGHT vector.
Vector features: CMV, Human cytomegalovirus immediate-early enhancer/promoter; QBI SP163, translational enhancer; 6xHis, epitope of 6 repeted Histidines for His antibody; EK recognition site, Enterokinase recognition site (allows removal of N-terminal tag); Amp, gene for ampicillin resistance; pUC origin, allows high copy number in E.coli; BGH pA, Bovine growth hormone polyadenylation signal; TRE-TIGHT modified TET-response element; Hyg, gene for hygromycin resistance; MoMuSV LTR, Moloney murine leukemia virus long terminal repeat; Extended Packaging Signal.

3.1.4 Transient transfection

Cells were transfected with Fugene 6, a cationic lipid based transfection reagent (Roche). Cells were seeded 14-18 hours prior to transfection to reach ~60% confluency. Appropriate DNA and Fugene 6 reagent were mixed according to manufacturer's instructions and incubated for 20-30 min. Cells were incubated with transfection mix for 10-12 hours before the media were changed and incubated for 48 hours. Transfections were done on 10 cm plates using 5µg vector DNA for samples to Western analyses and on 6 well plates using 1µg vector DNA for samples to qPCR.

Transfection of 3T3-L1 cells prior to induction of differentiation was done first at 3 days and then a second time 12 hours prior to induction. The second transfection was done because pilot experiments had shown that levels of ectopic expressed His-VHR diminish before the fourth day after transfection (data not shown) and we wanted to maintain the expression at least past the observed downregulation at day 4 and 6 in Figure 6B and C.

3.1.5 β-gal staining

β-gal staining was performed to check the efficiency of Fugene 6 transfections. Cells were transfected with pCMV β-gal (ATCC), treated with fix solution [2% formaldehyde (Sigma) and 0.2% gluteraldehyd in phosphate buffered saline (PBS)] and then incubated with histochemical stain [5mM potassium ferricyanide (Sigma), 5mM potassium ferrocyanide (Sigma), 2mM $MgCl_2$ (Sigma) and 1mg/mL X-gal (Saveen Werner) in PBS] at 37C for 14-24 hours. The pCMV β-gal vector contains the gene for β-galactosidase under the regulation of the minimal cytomegalovirus (CMV) promoter. Cells expressing the vector would be able to catalyze X-gal to a blue byproduct. Picture was taken with camera.

3.1.6 The TETON system

The used TETON system consisted of two vectors pREVTETON (Clonetech) and pREVTRE-TIGHT. The latter was constructed by former lab member Piotr Kurys by

cutting the TIGHT element from the commercially available pTRE-TIGHT and pasting it into the pREVTRE construct. pREVTETON express the reverse tetracycline-controlled transactivator (rtTA) from CMV promoter. In the presence of Tc, or a derivate (e.g. dox), the rtTA binds to a TET-response element (TRE) located upstream of a CMV promoter on pREVTET-TIGHT and induces expression of the gene of interest inserted downstream of the CMV promoter. The TIGHT element of pREVTRE-TIGHT was inserted to ensure less transcription leakage from the vector in absence of Tc or dox. pREVTETON and pREVTRE-TIGHT are both retroviral vectors containing viral packing signal (Ψ^+) and long terminal repeats (LTR) but lack genes for core structural proteins (gag), reverse transcriptase/integrase (pol) and coat glycoproteins (env) [168]. Packaging cells (BOSC) expressing these three genes are used to produce infectious [169], but replication-incompetent retroviral particles which can then be used to infect other cells (see 3.1.10).

3.1.7 Luciferase assay

The pREVTRE-LUC (Clonetech) vector has a luciferase reporter gene downstream of the TRE controlled CMV promoter. Isolated 3T3-L1 clones were grown to 50-70% confluency on 12 well plates and transfected with 250 ng pREVTRE-LUC and 250 ng carrier DNA followed by 48h of treatment with or without 1µg/mL dox (Sigma) in media. Cells were then treated with lysis buffer [25mM Tris-HCl (both from VWR) (ph 7.8), 2mM DTT (Sigma), 10% glycerol (Invitrogen), 1% Triton-X (Sigma)], harvested and centrifuged at 15 000 g for 2 minutes. Supernatant was measured for luciferase activity with Victor^2 multilabel counter (PerkinElmer) where reaction buffer was added. The luciferase activity given in counts per second (CPS) was normalized to the protein concentration of the supernatant and compared to negative control.

3.1.8 cDNA synthesis and quantitative PCR

RNA was isolated from harvested cells using TRIzol (Invitrogen) and treated with DNase I (Ambion). cDNA was generated from 3µg RNA using SuperScript II Reverse Transcriptase (Invtrogen). Quantitative Polymerase Chain Reaction (qPCR)

was done, to measure cDNA levels of the MKPs and empty vector, using the LightCycler 480 system (Roche). In a reaction volume of 10µL 1x LightCycler480 SYBR Green I Master mix (Roche), 0.5µM of each primer and 1µL of cDNA template was mixed. Negative controls without template or with RNA, were also included in the reaction. The qPCR reaction was initialized with a 10 minutes enzyme hot-start/template denature step at 95°C. Next the reaction went through 40 cycles of 95°C denaturation for 10 seconds, primer dependent temperature (see Table 2) of annealing for 10 seconds, and 72°C extension for 20 seconds. The last cycle was followed by a melting curve analysis to ensure that a reaction free of byproducts had been performed. Dilution standard curves were used as external standards. The level of fluorescence emitted from SYBR Green dye when incorporated in double-stranded DNA, was detected in each cycle by the LightCycler 480 instrument. The crossing point (CP) values, defined as the point which the fluorescence increased appreciably above the background, gave values correlating to the total amount of cDNA in each of the samples. The CP values were used to calculate the relative expression of the genes of interest, comparing their values to those of the empty vector samples. All gene quantities were normalized to the murine housekeeping gene 36B4. Raw data were compiled with LightCycler 480 instrument software (Roche) and further data analyses were performed with Office Excel 2007 (Microsoft).

Name	Sequence	Anneal temp (°C)	Product length (bp)
mVHR	Forward: 5´-cgtctgtggctcaggacatc-3´	62	439
	Reverse: 5´-cattgagctggcagagttgg-3´		
hisMKP6	Forward: 5´-ggctagcatgactggtgga-3´	62	150
	Reverse: 5´-atgcctcctatgtctccc-3´		
mVH5	Forward: 5´-caaggatctgatgacccaaa-3´	64	87
	Reverse: 5´-cggctctcacagatgaagtc-3´		
36B4	Forward: 5´-aagcgcgtcctggcattgtct-3´	62	136
	Reverse: 5´-ccgcaggggcagcagtggt-3´		

Table 2. **Primers used in qPCR with sequences, annealing temperatures and product lengths**. All primers were purchased from Sigma.

3.1.9 Western analysis

Protein extracts were obtained from harvested cells by resuspending the cells in lysis buffer [0.5mM DTT, 20mM β-glycerol phosphate, 0.1mM $NaVO_3$, 2µg/mL Leupeptin, 1mM phenylmethylsulphonyl-fluoride (PMSF), 0.2M Hepes (pH 7.7), 3M NaCl, 2mM EDTA, 1% Triton-X, 15mM $MgCl_2$ (all from Sigma)] and rotating at 4°C overnight, followed by centrifugation at 15 000g for 20 minutes, 4°C. Protein concentration was measured with Victor^2 multilabel counter using Bio-Rad protein assay. Samples of 70µg protein were mixed with reducing SDS-buffer [187.5mM Tris-HCl (ph 6.8), 6% SDS (Fluka), 30% glycerol, 0.03% phenol red (Sigma), 1.25M DTT] and resolved through 10 % or 12% SDS-PA Gel. A Precision Plus Protein dual color ladder marker (Bio-Rad) determined the molecular weight of the bands. The proteins were transferred from the gel to a PVDF membrane (Bio-Rad). The membrane was blocked with 5% dry skimmed milk in TBST solution [Tris Buffered Saline (ph 7.4), 0.1% Tween (Sigma)] and incubated with primary antibody in TBST containing 5% BSA and 0.04% sodiumazide (Sigma) over night at 4°C. Primary antibodies used: anti (α)- His-tag mouse monoclonal antibody (1:5000 dilution, Clonetech), α-β-actin mouse monoclonal antibody (1:10000, Sigma), α-VHR rabbit polyclonal antibody (1:1000,), α-DUSP14 (MKP6 human homolog) goat polyclonal antibody (1:1000, abcam) , α-DUSP8 (VH5 human homolog) goat polyclonal antibody (1:1000, abcam), α-aP2 rabbit polyclonal antibody (1:2000, generous gift from Gökhan Hotamisligil), α-phospho-ERK rabbit polyclonal antibody (1:1000, Cell Signaling) , α-total ERK rabbit polyclonal antibody (1:1000, Cell Signaling). The membrane was incubated with secondary antibody in 5% milk TBST for 1 hour at room temperature. Secondary antibodies used: horseradish peroxidise-conjugated (HRP) α-mouse IgG antibody (1:5000, Sigma), HRP α-rabbit IgG antibody (1:10000, Sigma), HRP α-goat IgG antibody (1:8000, Santa Cruze Biotechnology). ECL Western blotting detection reagents and analysis system were utilized for the immunoreactive bands according to the manufacturer's (GE Healthcare) instructions. For quantification, Western blots were digitalized with scanner machine (Epson Perfection V700 Photo) and optical density was measured with the software ImageQuant TL (Amersham Biosciences).

3.1.10 Retrovirus production and infection

Virus packing BOSC cells were transfected with pREVTETON, pREVTRE-TIGHT, or pREVTRE-TIGHT His-VHR using Fugene 6. 48 hours after transfection virus containing media were collected and filtered through 0.45µm sterile filter. ~60% confluent 3T3-L1 cells grown for 14-18 hours were infected with a mix of 2 parts virus containing medium, 1 part standard medium, mixed with polybrene to a total concentration of 4µg/mL and incubated for 24 hours, after which cells were changed to standard medium and incubated for additional 48 hours. 3 days after infection start, cells were subjected to selection treatment (1000µg/mL G418 for pREVTETON infection of 3T3-L1 and 500 µg/mL G418 plus 300µg/mL Hygromycin for pREVTRE-TIGHT/pREVTRE-TIGHT His-VHR infection of 3T3-L1 TETON stable cell line) for 3 weeks. Healthy looking colonies were picked and expanded separately with half selection treatment.

3.1.11 Statistics

Statistical analyses were performed using the T-test in MS Excel. Values of $p < 0.05$ for 2-tailed T-test were considered significant.

4. Results

4.1 Regulation of VHR protein expression during 3T3-L1 differentiation

Previous finding in the Saatcioglu group have shown that several MKPs are regulated at the transcriptional level during adipogenic conversion of 3T3-L1 cells (Figure 5).

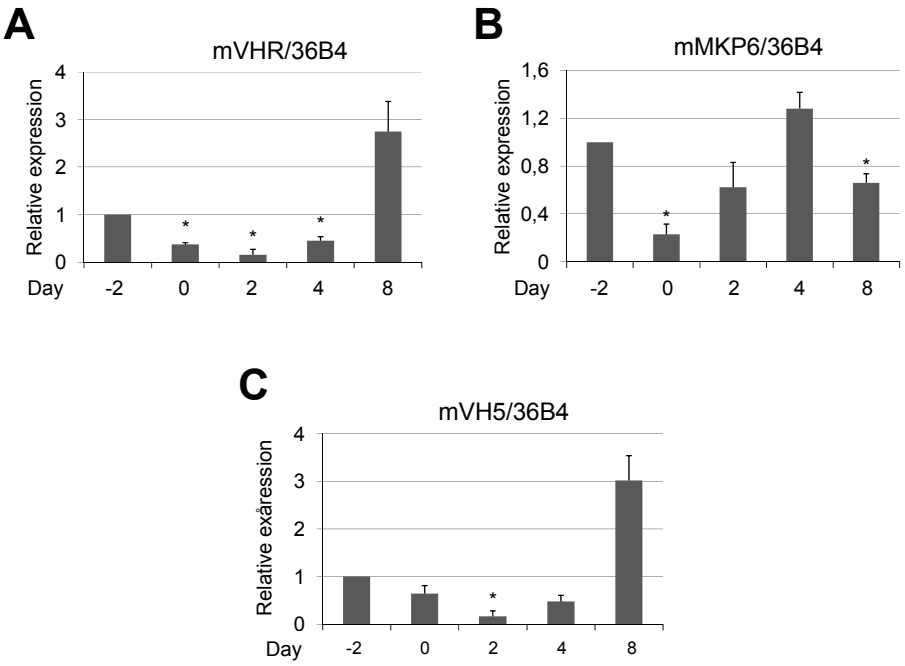

Figure 5. **MKP mRNA levels during differentiation of 3T3-L1 cells**. 3T3-L1 cells were induced to differentiate and harvested at indicated timepoints. Total RNA was isolated, converted to cDNA and expression of VHR (**A**), MKP6 (**B**) and VH5 (**C**) mRNA were measured by qPCR described in Materials and Methods. mRNA levels were normalized to 36B4 mRNA and are presented relative to day -2 samples. The results presented are the average of three independent experiments. * indicates significance compared to day -2 samples, $p < 0.05$, $n = 9$.

To confirm the significance of these data we chose the three most significantly regulated MKPs, VHR, MKP6 and VH5, for further studies. 3T3-L1 cells were induced to differentiate and harvested at time-points as shown in Figure 6B and C. Since there is a report indicating MKP1 action in hypertrophied 3T3-L1 cells [167], we additionally looked at protein levels in the hypertrophied state. Differentiation was confirmed by Oil Red O staining of TG accumulated in developed (day 8) and hypertrophied (day 21) adipocytes (Figure 6A). Unfortunately, due to problems with antibodies for MKP6 and VH5 no conclusive results on endogenous protein levels

during adipogenesis could be obtained. However, Figure 6B shows quantification from Western analysis with VHR antibody from two separate differentiation experiments. VHR expression is significantly downregulated up to day 6 followed by a significant upregulation into the hypertrophied state at day 16. Figure 6C shows a representative Western blot for VHR expression with β-actin levels as loading control. We therefore conclude that VHR expression is downregulated in the beginning stages of differentiation up to day 6, but upregulated thereafter exceeding the day 0 levels at day 12, and reaching maximal levels by day 16. These data are consistent with the mRNA data of VHR in Figure 5A.

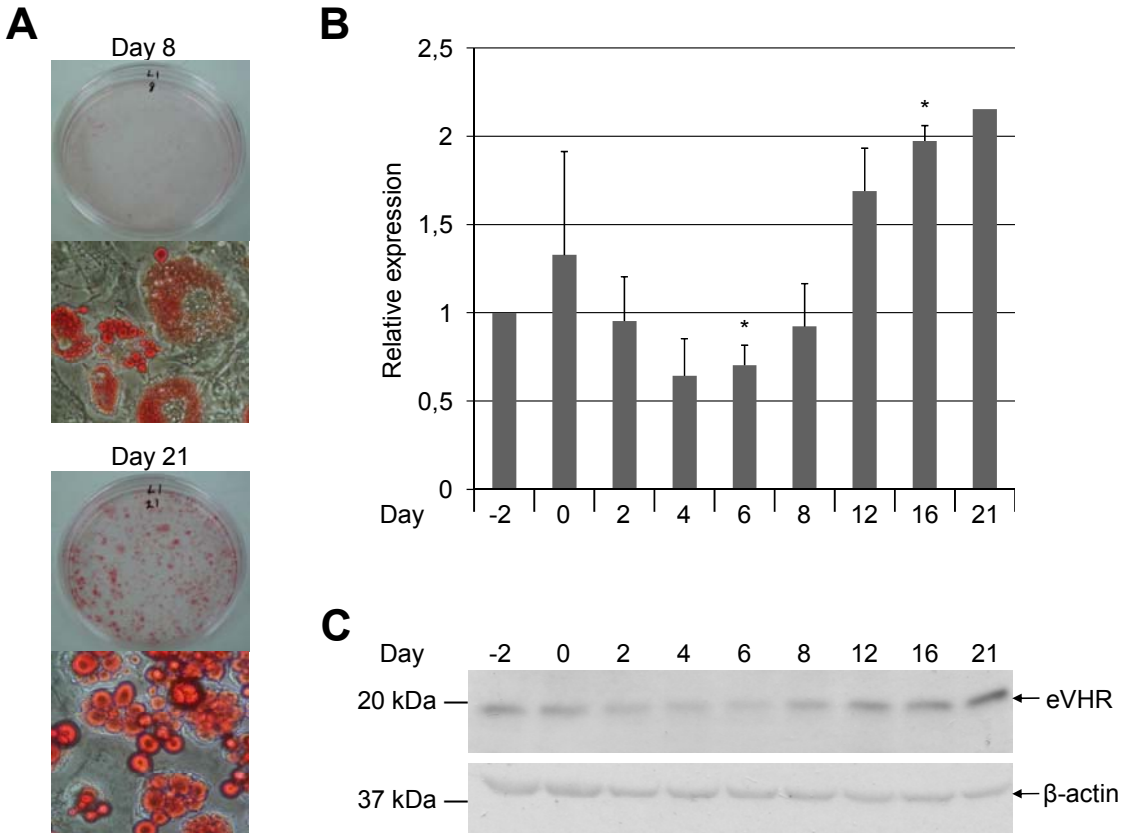

Figure 6. **VHR protein levels during 3T3-L1 differentiation**. Proliferating 3T3-L1 cells (-2) were grown to confluency. Two days post confluency (0) cells were subjected to induction medium described in Materials and Methods and then stained with Oil Red O or harvested at indicated timepoints. Harvested cells were subjected to protein extraction for Western analysis. **A**: Differentiation status was verified with Oil Red O staining, displaying mature (day 8) and hypertrophied (day 21) 3T3-L1 cells magnified 1X and 200X. **B**: Four separated Westerns analysis for VHR expression, obtained form two independent differentiation experiments were quantified by optical density described in Materials and Methods. The quantified data were normalized to quantification of β-actin levels for correnponding timepoint and are presented relative to day -2. * indicate significance, $p < 0.05$, $n = 4$, except day 21 with $n = 1$. **C**: A representative blot for the four Western analyses probed for VHR antibody is indicated (eVHR). β-actin was used as loading control.

4.2 Ectopic expression of MKPs

In order to study the functional role of the three MKPs chosen, we constructed mammalian expression vectors for them. VHR and MKP6 vectors were made by other lab members while VH5 cloning was part of this work. For all vectors the MKP open reading frame was cloned into the pcDNA4 expression vector with a His tag in the 5' end to facilitate its detection in further applications. The His-MKP fragment was then transferred to a pRevTRE-TIGHT construct which enables retroviral expression in a Tc inducible manner. Tc-inducible systems require the simultaneous expression in the same cell of the Tc-dependent Activator protein along with the Tc (dox)-inducible constructs [170].

To confirm successful construction of the various MKP constructs, 3T3-L1 and COS-7 cells were transiently transfected with either a pcDNA4 MKP or a pRevTRE-TIGHT His-MKP, referred to as pcMKP and tetMKP, respectively, from now. Figure 7A shows the mRNA levels of ectopically expressed VHR in 3T3-L1 cells in which expression was approximately 15-fold higher in the pcDNA4 compared with the TETON system. Treatment with dox induced 3T3-L1 tetVHR ~9-fold compared to non-treated cells. Leakage from the TETON system is a common problem [171] but that does not seem to be the case here. Western analysis with a His antibody shows that protein expression correlates with mRNA expression in both 3T3-L1 cells (Figure 7B) and COS-7 cells (Figure 7C) confirming that both constructs are functional in both cell lines.

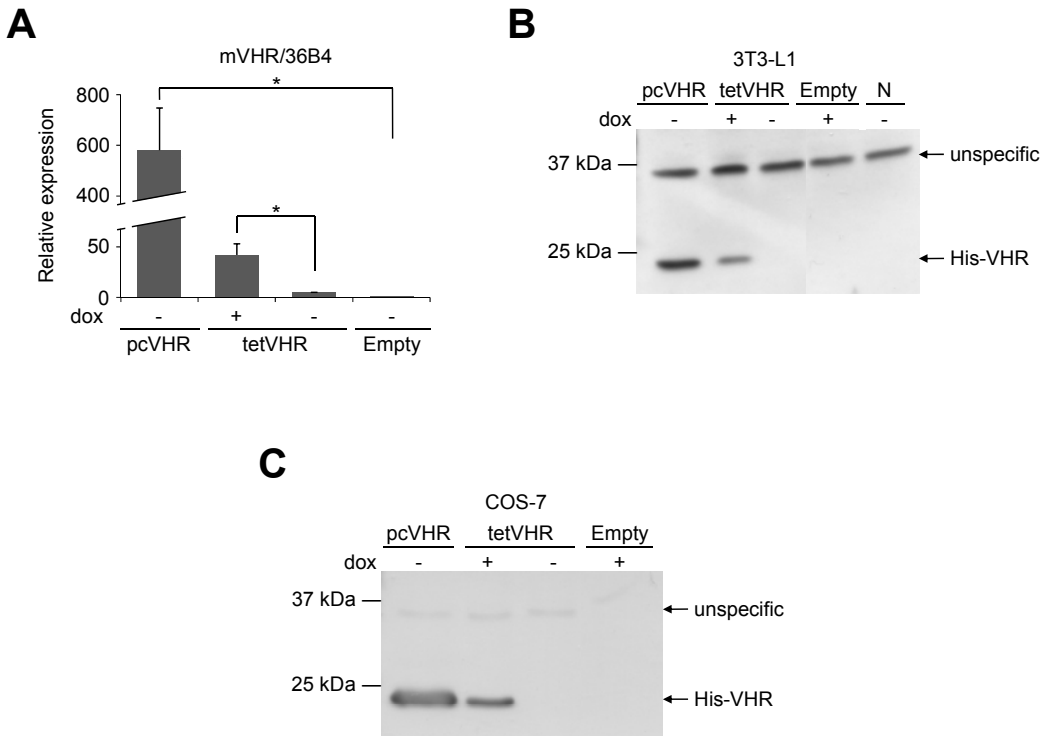

Figure 7. **Ectopic expression of VHR in 3T3-L1 and COS-7 cells.** 3T3-L1 and COS-7 cells were transfected with pcVHR, tetVHR+rtTA, empty vector or left untransfected (N). Cells were then incubated with or without dox as indicated. Cells were harvested, mRNA or protein extracts were prepared, and were used in qPCR or Western analysis. **A**: mRNA expression of VHR in 3T3-L1 cells was determined by qPCR as detailed in Materials and Methods. Levels were normalized to 36B4 mRNA and are presented relative to empty vector. * indicates significance, $p < 0.05$, $n = 3$. **B**: Expressed His-VHR protein was detected by Western analysis of 3T3-L1 whole cell extracts probed for His antibody. An unspecific band used as loading control is indicated (unspecific). **C**: Expressed His-VHR protein was detected by Western analysis of COS-7 whole cell extracts probed for His antibody. An unspecific band used as loading control is indicated (unspecific).

A similar analysis was carried out for MKP6 as shown in Figure 8. As with VHR, pcMKP6 construct gave rise to significantly higher mRNA expression, approximately 60-fold more than that observed with tetVHR. Nevertheless, there was strong dox regulation of VHR expression from tetVHR with a 14 fold upregulation in the presence of dox. Figure 8B verifiy that the His antibody recognizes the expressed His-MKP6 protein. While ending this work, a new commercial antibody against human DUSP14 became available. According to manufacturer, sequence alignment indicated that this antibody may also have specificity against the murine MKP6. Figure 8C and D show both the transfected and endogenous MKP6 detected with this antibody. pcMKP6 expression is high and the dox induced tetMKP6 is apparent. No

visible band is seen without addition of dox. As seen with the VHR constructs, the MKP6 constructs work in both 3T3-L1 and COS-7 cells.

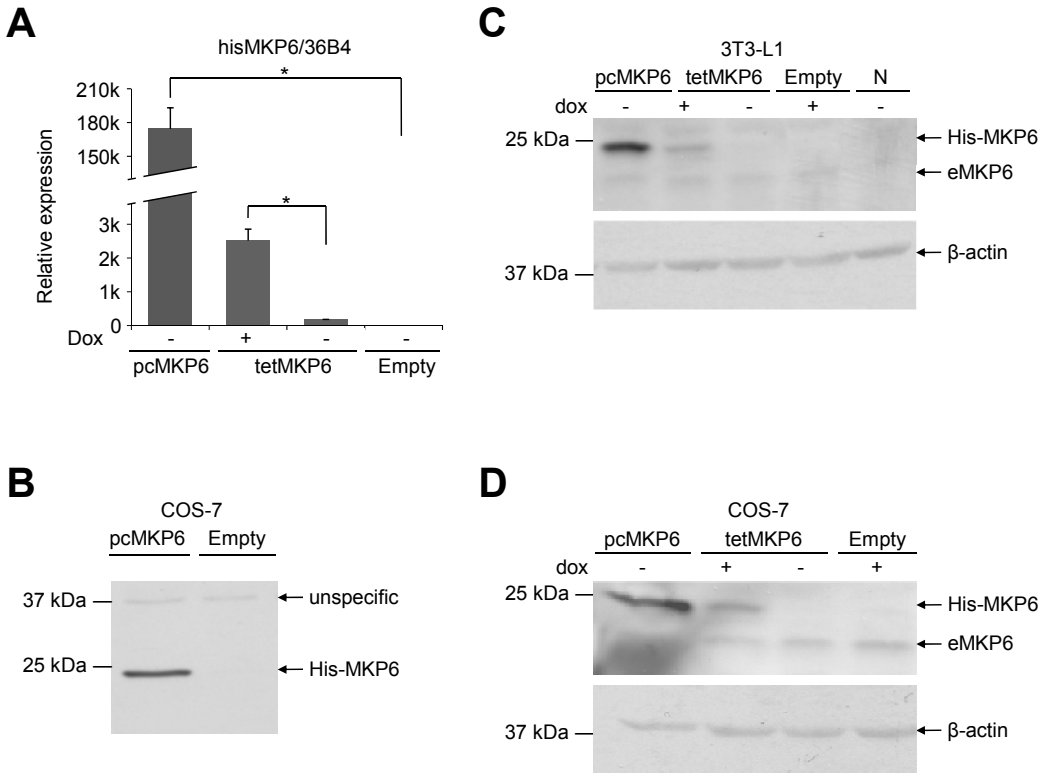

Figure 8. **Ectopic expression of MKP6 in 3T3-L1 and COS-7 cells.** 3T3-L1 and COS-7 cells were transfected with pcMKP6, tetMKP6 + rtTA, empty vector or left untransfected (N). Cells were then incubated with or without dox as indicated. Cells were harvested, mRNA or protein extracts were prepared, and were used in qPCR or Western analysis. **A**: mRNA expression of His-MKP6 in 3T3-L1 cells was determined by qPCR as detailed in Materials and Methods. Levels were normalized to 36B4 mRNA and are presented relative to empty vector. * indicates significance, $p < 0.05$, $n = 3$. **B**: Expressed His-MKP6 protein was detected by Western analysis of COS-7 cell extracts probed for His antibody. An unspecific band used as loading control is indicated (unspecific). **C**: Ectopically expressed (His-MKP6) and endogenous expressed (eMKP6) MKP6 was detected by Western analysis of 3T3-L1 cell extracts probed for DUSP14 antibody. β-actin was used as loading control. **D**: Ectopically expressed (His-MKP6) and endogenous expressed (eMKP6) MKP6 was detected by Western analysis of COS-7 cell extracts probed for DUSP14 antibody. β-actin was used as loading control.

A similar analysis was carried out for VH5 as shown in Figure 9. As with VHR and MKP6, the pcVH5 construct gave rise to significantly higher mRNA expression, approximately 10-fold more than that observed with tetVH5. There was strong dox regulation of VH5 expression from tetVH5 with a 7-fold upregulation in the presence of dox. The His antibody that was used for VHR and MKP6 (Figure 7 and 8) has proved difficult to use against His-VH5 since a strong unspecific band migrated to the same area as VH5 (data not shown). As with MKP6, a new antibody against human DUSP8 recently became available and was predicted, by manufacturer, to

bind murine VH5 as well. Figure 9B shows that both pcVH5 and tetVH5 specify expression of His-VH5 in COS-7 cells. Due to high unspecific binding, an endogenous VH5 expression could not be identified with the DUSP8 antibody.

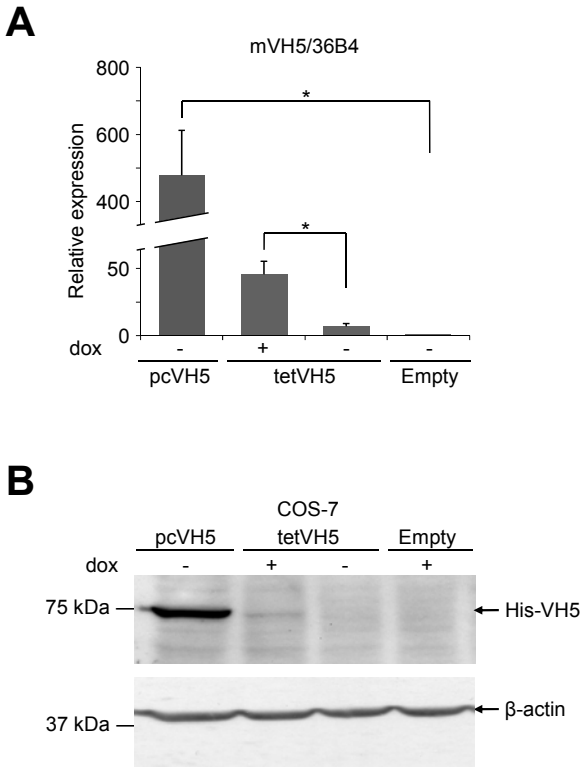

Figure 9. **Ectopic expression of VH5 in 3T3-L1 and COS-7 cells.** 3T3-L1 and COS-7 cells were transfected with pcVH5, tetVH5+rtTA or empty vector. Cells were then incubated with or without dox as indicated. Cells were harvested, mRNA or protein extracts were prepared, and were used in qPCR or Western analysis. **A**: mRNA expression of VH5 in 3T3-L1 cells was determined by qPCR as detailed in Materials and Methods. Levels were normalized to 36B4 mRNA and are presented relative to empty vector. * indicates significance, $p < 0.05$, $n = 3$. **B**: Expressed His-VH5 protein was detected by Western analysis of COS-7 cell extracts probed for DUSP8 antibody. β-actin was used as loading control.

4.3 Establishment of a stable 3T3-L1 TETON cell line

In order to induce expression of any protein of interest at any time during differentiation of 3T3-L1cells we decided to use the TETON system. As shown above, this system was functional in 3T3-L1 cells in transient transfection assays. To generate a stable TETON 3T3-L1 cell line, we infected 3T3-L1 cells with retrovirus packed in BOSC cells transfected with the pRevTetON vector that specifies expression of the rtTA protein. High transfection efficiency (80-90%) of BOSC cells was obtained (data not shown) indicating good virus production. After infection, the cells were subjected to selection with G418. 48 colonies formed under this selection over a period of 3 weeks were picked and expanded, 41 clones proved viable. Clone numbering started at 25 to prevent mix-up with sample data from earlier attempts to establish 3T3-TETON cell line in the group. Expanded clones were screened for dox responsiveness using a luciferase reporter assay in which the expression of luciferase is under the control of TRE binding sites [172]. Results from selected clones are shown in Figure 10A which indicated that clone #26 was a possible 3T3-L1 TETON stable cell line, with a dox-induced activity of ~6 times higher than that of the non-induced cells. The 3T3-L1 TETON clone #26 will from now on be referred to as 3T3-tetON26.

Luciferase activity of non-induced controls in Figure 10A was high for all clones compared to the induced and in a few cases higher (most likely caused by a combination of leakiness and unstable transfection efficiency). In an attempt to reduce the background luciferase expression in non-induced cells, Tc depleted medium was used in an independent experiment to confirm the initial results from Figure 10A. In addition, different amounts of luciferase vector were used for optimization. Data presented in Figure 10B correlates with the results of Figure 10A, with a significant ($p < 0.05$) increase of luciferase activity for dox treated cells when 250 ng of luciferase vector was used. Transfecting cells with 50 ng luciferase vector seemed inefficient as activity for both induced and non-induced cells were low. Using 100 ng of luciferase vector gave a bit lower un-induced response and higher dox-

induced response than the 250 ng transfection, but great difference in the induced luciferase activity, making it non-significant. In summary, we estimate that the 3T3-tetON26 clone has 3.5–6 fold inducibility when treated with dox. Although this is less than optimal, we decided to work further with this clone.

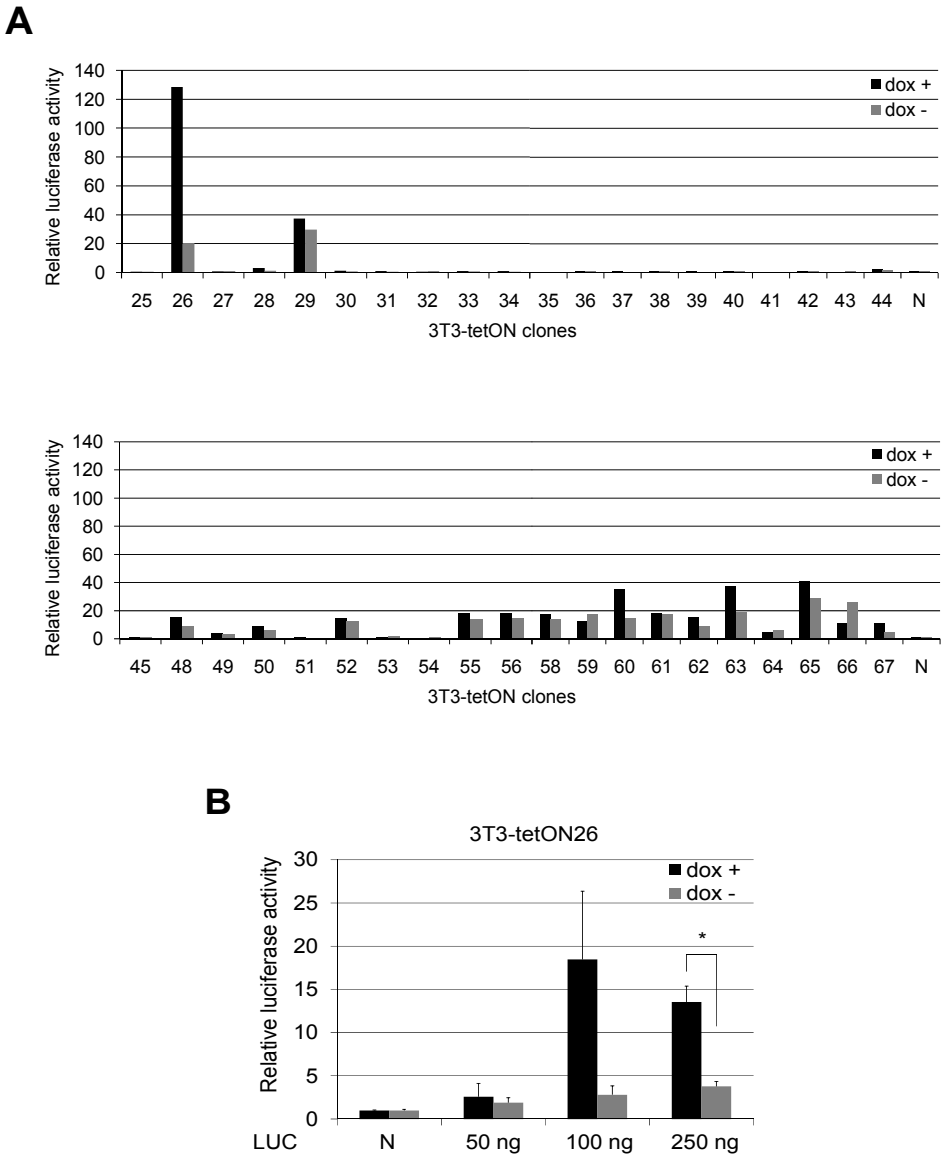

Figure 10. **Screening of 3T3-L1 TETON clones**. **A**: Represented clones were grown to 50-70% confluency on 12 well plates with standard media and transfected with 250 ng pREVTRE-LUC and 250 ng carrier DNA and treated with or with out dox. Untransfected cells were used as negative control (N). Cells were treated with lysis buffer, harvested and subjected to luciferase assay analysis described in Materials and Methods. The graphs present an average of the measured luciferase activity from 2 separate transfections set relative to negative control. **B**: Clone 26 cells were grown to 70% confluency on 12 well plates with Tc depleted media and cotransfected with 50 ng, 100 ng or 250 ng pREVTRE-LUC indicated (LUC) and carrier DNA to a total of 500 ng. Untransfected cells were used as negative control (N). Cells were treated with or without dox, treated with lysis buffer, harvested and subjected to luciferase assay analysis. Luciferase activity of dox induced cells was set reative to activity of negative control. * indicate significance, $p < 0.05$, $n = 3$.

4.4 Establishment of a stable 3T3-L1 TETON TRE-TIGHT His-VHR cell line

Having made an inducible 3T3-L1 TETON cell line, we first set out to make an inducible cell line for His-VHR. 3T3-tetON26 cells were infected with retrovirus harboring the tetVHR vector. 15 colonies were picked and expanded. Only 8 clones were viable. These were screened for His-VHR expression by Western analysis. Figure 11A shows the initial screen of 4 of the 8 clones. 3T3-tetON26 tetVHR8 (VHR8 in Figure 11A) showed expression levels similar to expression with pcVHR. This clone is named 3T3-tetVHR8. Expression in the non-induced cells were low and expression in all the other clones were absent, with the exception of VHR5, where low level of VHR was detected in the presence of dox.

To confirm these initial findings, and to compare the induced expression of His-VHR relative to endogenous VHR expression, 3T3-tetVHR8 cells were cultured with or without dox. Total cell protein extracts were prepared and subjected to Western analysis with a VHR antibody (Figure 11B). In this experiment the inducibility of tetVHR was lower than in the first experiments (Figure 11A). Furthermore, expression of His-VHR was lower than the endogenous VHR (eVHR). Surprisingly, endogenous VHR expression in the 3T3-tetVHR8 cells was markedly increased compared with the negative and the positive control cell lines.

To check whether the elevated endogenous VHR levels are transient in 3T3-tetVHR8 cells, a third check of dox inducibility was done after 5 passages. In addition, both Tc depleted medium and standard medium were used to look for an effect in the non-induced expression of His-VHR. We also transiently transfected the 3T3-tetVHR8 cells with either tetVHR or pRevTetON in an attempt to increase in His-VHR expression increasing rtTA or tetVHR gene. A potential increase compared to the dox-treated 3T3-tetVHR8 cells could indicate that one of the virally introduced genes had stunted transcription. Figure 11C shows that endogenous levels of VHR in the VHR8 clone is still considerably higher than in the original 3T3-L1 cell (E). The His-VHR expression is still inducible and no apparent difference in the use of Tc depleted

medium compared with standard medium is observed. Transient transfection of 3T3-tetVHR8 did not affect the expression of His-VHR. We thus conclude that with higher expression of endogenous VHR than induced His-VHR, the 3T3-tetVHR8 cells are unfortunately not suitable for our experiments.

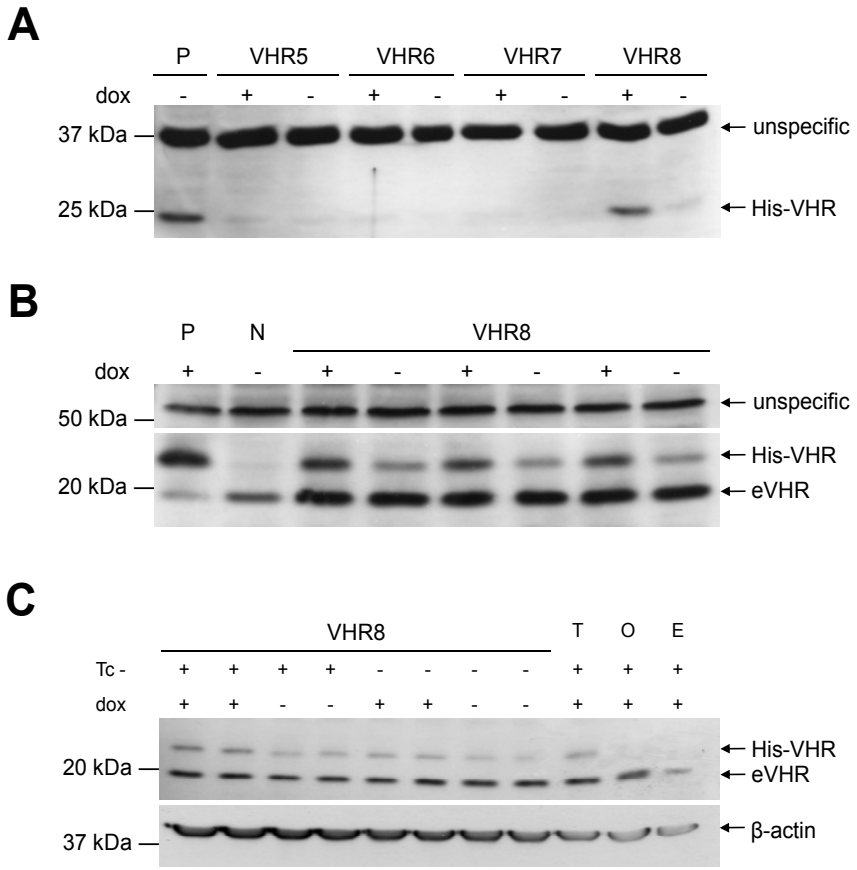

Figure 11. **Screening of 3T3-L1 TETON TRE-TIGHT VHR clones. A**: Whole cell extracts were prepared from representative clones (VHR5-8) grown to 50-70% confluency and induced with dox and used in Western analysis with a His antibody. An unspecific band used as loading control is indicated (unspecific). P indicates extracts prepared from 3T3-L1 cells transfected with pcVHR. **B**: VHR8 cells were grown to ~70% confluency and were either left untreated or treated with dox. Whole cell extracts were prepared and subjected to Western analysis with VHR antibody (eVHR indicates endogenous VHR and His-VHR indicates induced expression). An unspecific band used as loading control is indicated (unspecific). P indicates extracts prepared from 3T3-L1 cells transfected with pcVHR. N indicates extracts prepared from 3T3-L1 cells transfected with an empty vector. **C**: VHR8 cells were grown to ~70% confluency in Tc depleted (Tc-) or standard medium and were either left untreated or treated with dox. Whole cell extracts were prepared and subjected to Western analysis with VHR antibody (eVHR indicates endogenous VHR and His-VHR indicates induced expression). Antibody against β-actin was used as loading control. T = VHR8 ectopic expressing pRevTRE-TIGHT 6HisVHR. O = VHR8 ectopic expressing pRevTetOn and. E = 3T3-L1 empty vector.

4.5 ERK activation immediately after induction of differentiation.

Prior to this work one publication has investigated the early dynamics of ERK phosphorylation in differentiation of 3T3-L1 cells [119]. We wanted to confirm these data. 3T3-L1 cells were induced to differentiate and were harvested at different timepoints before and after induction. Whole cell extracts were prepared and subjected to Western analysis with antibodies recognizing phosphorylated ERK and total ERK (Figure 12). There was a quick burst of phosphorylation of ERK immediately after induction. Phosphorylation started to diminish within 30 minutes after induction and is heavily reduced after 2 hours. Worth noting is the slightly elevated ERK2 phosphorylation after 12 hours. These findings are in general agreement with previously published data [119], although the phosphorylation burst that they observe after after 12 hours is stronger. In the un-induced growth arrested 3T3-L1 cells (timepoint 0) we observed ERK activation compared to proliferating cells (timepoint -2). This deviated from what was previously reported where there low ERK activity and no phosphorylation differences between growth arrested and proliferating cell was seen [119]. We do not know the basis for these minor differences between our data and those that were published previously.

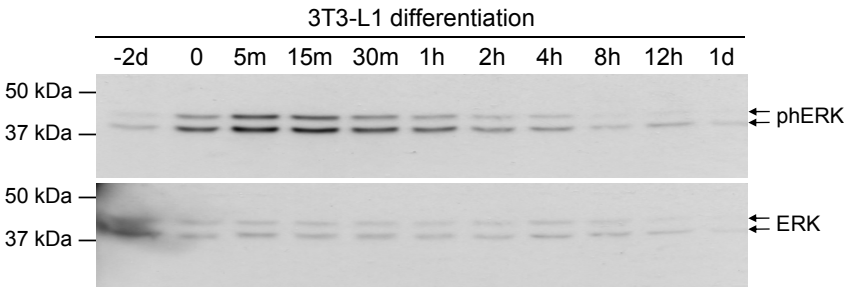

Figure 12. **ERK1/2 activity in 3T3-L1 cells after induction of differentiation.** Proliferating 3T3-L1 cells (-2d) were grown to confluency. Two days post confluency (0) cells were subjected to induction medium (described in Materials and Methods) and then harvested at indicated timepoints (m = minutes, h = hours, d = days). Whole cell extracts were prepared and subjected to Western analysis with phopho-ERK antibody (phERK indicates phosphorylation levesl of ERK1 and ERK2, upper and lower bands respectively). Total ERK levels are used as loading control (ERK).

4.6 His-VHR overexpression prior to and during 3T3-L1 differentiation

Since the 3T3-tetVHR8 clone had significantly elevated endogenous levels of VHR, we decided to study the impact of VHR expression on MAPK phosphorylation by transiently transfection of pcVHR into 3T3-L1 cells. pcVHR or an empty expression vector were transfected into 3T3-L1 cells which were then differentiated. Cells were harvested at different timepoints and whole cell extracts were prepared and subjected to Western analysis with different antibodies. Un-transfected 3T3-L1 cells were used as control of final differentiation status.

As shown in Figure 13B, there were no observable differences in differentiation status of the VHR overexpressing 3T3-L1 cells compared with empty vector transfected or untransfected cells assessed by Oil Red O staining. Furthermore, there was similar aP2 expression (Figure 13A) in cells transfected with pcVHR and cells transfected with empty expression vector demonstrating that VHR does not affect the final differentiation status of the 3T3-L1 cells. Examination of ectopically expressed His-VHR indicated that it is present until day 8 although it weakens considerably during the course of differentiation as would be expected from a transiently expressed protein. There were no differences ERK phosphorylation for the His-VHR overexpressing cells and the cells transfected with empty vector (Figure 13A), indicating that VHR has no effect on ERK phosphorylation in 3T3-L1 cells. The trend for phosphorylation of ERK is similar in Figure 13A to that of Figure 12 with a quick transient burst seen immediately after induction. However, we clearly see some differences when comparing the empty expression vector transfected cell (Figure 13A) with the untransfected cell (Figure 12): the transfected proliferating 3T3-L1 cells (day -2) display much more phosphorylation than that in non-transfected cells; the opposite is observed in ERK activation in day 0. Furthermore, transfected cells in Figure 13A appear to maintain ERK phosphorylation longer after induction with equal levels of phosphorylation at timepoints 30 minutes and 2 hours, whereas in untransfected cells the 2 hour phosphorylation is lower than that at 30 minutes. This

may indicate an effect of the transfection scheme on ERK phosphorylation which should be considered while evaluating these data.

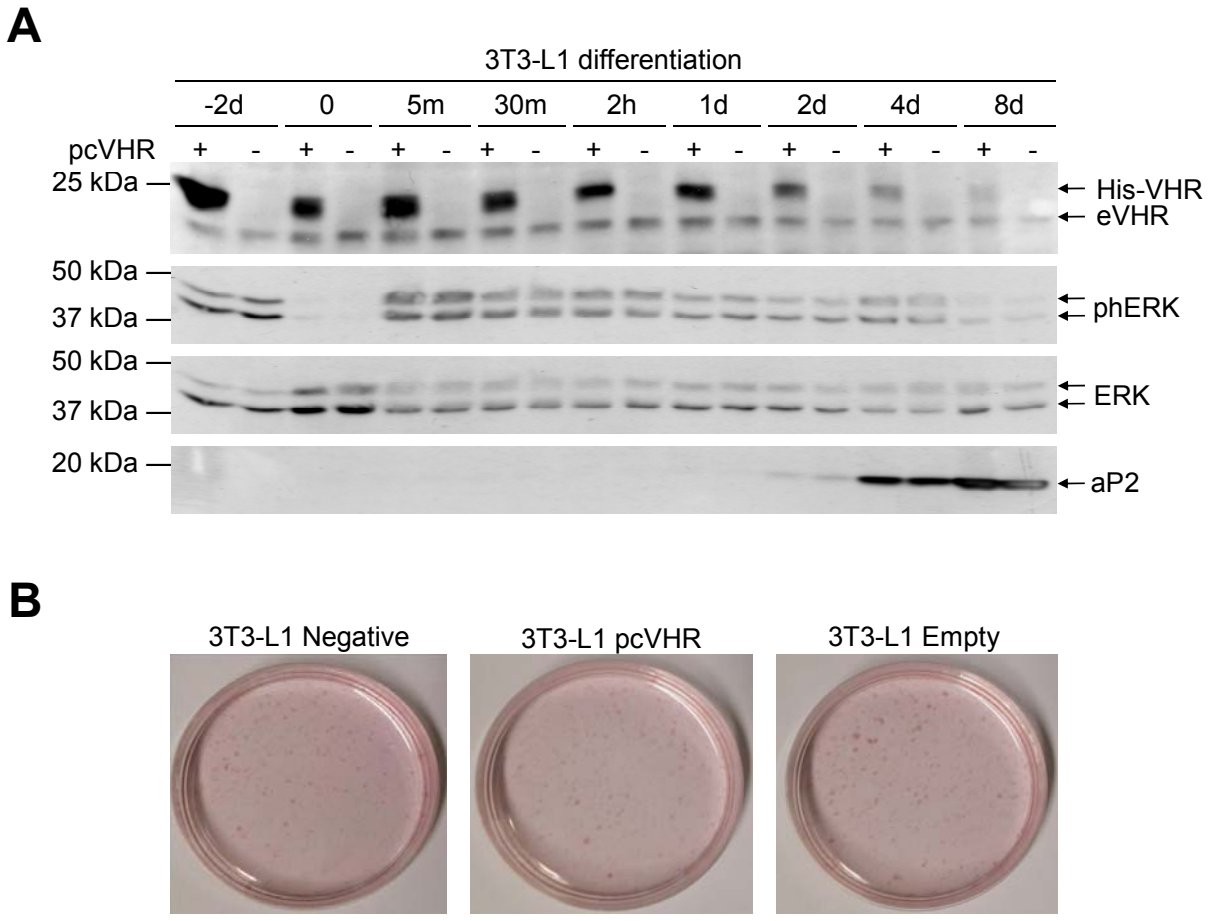

Figure 13. **Overexpression of His-VHR prior to and during 3T3-L1 differentiation.** 60% confluent 3T3-L1 cells were transfected first three days and secondly 12 hours prior to transfection with pcVHR (+) or empty vector (-) described in Materials and Methods. Cells were induced to differentiate two days after reached confluency and then harvested at indicated timepoints or stained with Oil Red O. **A**: Whole cell extracts were prepared from the indicated timepoints (m = minutes, h = hours, d = days) and used in Western analyses with VHR antibody (eVHR indicates endogenous VHR and His-VHR indicates induced expression). Western analysis with phospho-ERK antibody (phERK) indicates phosphorylation levels of ERK1 and ERK2, upper and lower bands respectively. Total ERK levels are used as loading control (ERK). Differentiation of His-VHR expressing cells and empty vector transfected cells were compared by Western analysis with aP2 antibody. **B**: Differentiation status of pcVHR and empty vector transfected and untransfected (Negative) cells 8 days post induction, were compared with Oil Red O staining.

5. Discussion

In this study, we have found that regulation of VHR protein expression during adipogenesis correlates with what we have observed earlier for mRNA levels (Figure 5A and 6B and C). VHR levels are down regulated at day 4-6 compared to the pre-adipogenic state and rise as the 3T3-L1 cells develop into mature adipocytes at day 8. Further culturing of the adipocytes leads to hypertrophy observed with an increase of lipid droplet size (Figure 6A) [167]; interestingly, VHR levels continue to rise into the hypertrophied state (Figure 6B and C). No data is yet obtained for MKP6 or VH5 regulation during adipogenesis at the protein level due to lack of a functional antibody during the course of this study. Work is in progress to optimize the conditions to use the available antibodies to detect endogenous MKP6 andVH5 (see below)

Through ectopic expression we have confirmed that the constructs for overexpression of the VHR, MKP6 and VH5 are transcribed into mRNAs and translated into proteins (Figure 7-9). These experiments also indicated that the human DUSP14/MKP6 and DUSP8/VH5 antibodies could be used as probes against the murine MKP6 and VH5 proteins, respectively (Figure 8C, 8D and 9B). We have found the conditions for the MKP6 antibody to get a distinct specific band also for endogenous MKP6 in 3T3-L1 cells (Figure 8C) which can now be used to investigate a possible regulation of the MKP6. On the other hand, we have not yet observed VH5 protein expression in 3T3-L1 cells. This may indicate a posttranscriptional regulation of VH5 in 3T3-L1 cells which results in the loss of the epitope that was used to raise the antibody, but is more likely to be low transfection efficiency and/or lack of specificity of the antibody (Figure 9B).

There are large differences in the expression of the MKPs from the pcDNA4/HISMax vector and the pRevTRE-TIGHT vector, especially observed for mRNA, reaching a 100-fold difference (Figure 7A-9A). These differences could be due to a combination of several factors. For example, the pcDNA4 MKP transfection experiments were performed with double the amount of expression vector compared with pREVTRE-

TIGHT transfections. In addition, the promoters that drive the expression of the MKPs in the two vectors are different (Figure 4).

By use of retroviral infection, we established a stable cell line expressing the rtTA factor (3T3-tetON26), confirmed by a luciferase reporter assay (Figure 10A and B). The fold induction of luciferase activity was less than what we observed with the transient expression studies (Figure 7A-9A). Nevertheless, we decided to work further with this clone, as the luciferase vector used in the luciferase assay lack the TIGHT element that is present in the tetMKP.

The second retroviral infection of the 3T3-tetON26 cell line resulted in a stable cell line able to induce expression of His-VHR in the presence of dox (3T3-tetVHR8, Figure 11A). Unfortunately, further tests of the 3T3-tetVHR8 revealed that His-VHR was also expressed without dox induction (Figure 11B and C). In addition, compared with wild type 3T3-L1 cells, endogenous VHR expression has been chronically elevated to a level higher than the induced expression of His-VHR (Figure 11B and C). The leaky His-VHR expression and the elevated endogenous VHR levels made this cell line not suitable for further investigations of VHR in 3T3-L1 adipogenesis. These findings made it necessary to recheck the endogenous levels of VHR in the 3T3-tet26 cell line to find out if the elevated levels of VHR were caused by the process of introducing His-VHR with retrovirus or in the first infection. Data not presented here show an increase in the endogenous levels of VHR in 3T3-tetON26 cells. This suggests that the process of infecting 3T3-L1 cells lead to elevated endogenous VHR levels. One possibility is that the isolated 3T3-tetON26 clone itself had higher VHR levels than the rest of the cell pool prior to infection for unknown reasons. This can be elucidated by comparing the endogenous VHR expression of the 3T3-tetON26 clone to other isolated clones from the same infection. Another scenario is that the selection of the 3T3-tetON cells with G418 was too high and stressed the cells to alter their VHR expression pattern. Earlier attempts in the group to establish a 3T3-L1-tetON cell line have used lower concentrations of G418 and could therefore be compared with 3T3-tetON26 cells to see if the selection scheme itself has an effect on VHR expression in the 3T3-L1 cells. The higher selection used in this study was

based on experience in previous selections where a large proportion of the picked colonies was false positive. Also higher selection tended to give greater rtTA expression in true positive stable clones.

Two previous studies have found early activation of ERK in 3T3-L1 cells after induction [119, 123]. Both publications report an immediate activation of ERK, followed by a rapid decline. Our data are largely in agreement with these findings (Figure 12 and 13A); there are, however, some differences. Figure 12 shows little ERK phosphorylation at day -2 and an incremental increase just prior to induction. Figure 13A displays quite high ERK phosphorylation at day -2 and a clear reduction at day 0. We do not know the basis for these differences. A recent publication showing that cationic lipids can induce ERK phosphorylation [173] support the hypothesis that the transfection reagent that was used itself could be the cause of the differences observed when comparing phospho ERK levels in Figures 12 and 13A. In contrast, previous studies display equal levels in ERK phosphorylation in proliferating and post confluent 3T3-L1 cells [119, 123]. These differences could be caused by cell line deviations, or indicate fluctuating ERK phosphorylation in proliferating cells which is abolished when cells go into growth arrest. Following this hypothesis, our post confluent cells (day 0) in Figure 12 may not have entered growth arrest completely and this could explain the elevated ERK phosphorylation compared to cells in Figure 13A (day 0).

ERK and JNK have been found as substrates for dephosphorylation by VHR both *in vitro* and *in vivo* [155, 174, 175]. VHR also has a proposed role in cell cycle progression [158], making it highly interesting to study its possible role in adipogenesis. Ectopic expression of VHR alone does not affect ERK phosphorylation during adipogenesis of 3T3-L1 cells (Figure 13A). Neither does the ectopic expressed VHR affect the lipid accumulation and aP2 expression, both markers of differentiation (Figure 13A and B). One could argue that the tagged VHR that we express does not have wild type enzymatic activity. For example, the His tag at the N-terminus of VHR could potentially inhibit its phosphatase activity. However, earlier reports have shown that an HA-tag at the N-terminus, a much larger tag, did

not affect VHR enzyme activity [155], and thus this is unlikely to be the reason for the lack of effect of VHR expression on ERK activity in 3T3-L1 cells. Another possibility is that lack of appropriate activators of VHR in 3T3-L1 cells hinders its activity on ERK. For example, VRK3 and Zap-70 have been identified as activators of VHR necessary for ERK dephosphorylation [156, 157]. It is possible that one or both of these factors is lacking or dimished in 3T3-L1 cells and that is the basis for lack of VHR activity towards ERK.

It should be considered that VHR may still exert effects in adipocytes or developing adipocytes without affecting aP2 expression and lipid accumulation. The elevated VHR levels from day 8 to day 21 of 3T3-L1 differentiation (Figure 6B and C) could suggest a role in hypertrophied state of these cells. Other targets of VHR, both known and unknown, may be modified and may contribute to this phenotype. For example, VHR overexpression can affect JNK activity which should definitely be checked since JNK activation is associated with hypertrophy of adipocytes, but not adipogenesis per se [122, 133]. The role of VHR in cell cycle regulation is also relevant here since in adipogenesis proliferation and growth arrest play important roles [53, 61]. Although overexpression may not particularly affect the cell cycle, knockdown experiments (using siRNA) or inactivation (using inhibitors) of VHR in 3T3-L1 cells would make it possible to investigate its role in adipogenesis.

With the constructs and antibodies for MKP6 and VH5 in places (VH5 antibody needs some more optimization), similar analysis on them can be performed. To investigate the overexpression of MKPs in the later stages of adipogenesis of 3T3-L1 cells or in hypertrophied state, transient transfection would be inefficient. A new attempt to establish a TETON 3T3-L1 cell line is warranted that gives a larger fold increase in response to dox. To our knowledge, there are no reports to date of a successfully established 3T3-L1 TETON cell line. Two groups have used the TetOFF system (opposite of TETON: Tc/dox inhibits expression) in 3T3-L1 cells [176, 177] and this can be adopted. Another alternative could be establishing a 3T3-L1 cell line stably expressing the coxsackievirus and adenovirus receptor (CAR) which enhance the transduction efficiency of the cell line for adenovirus [178, 179] that would make

these cells amenable for adenoviral transduction. Finally, generation of VHR knockdown mice, especially those in which the knockdown is targeted in fat tissue, would be a very useful experiments to conclusively assess the role of VHR in adipogenesis.

In summary, the data presented here suggest that VHR may have a role in adipogenesis. Further studies, involving both overexpression and knockdown of VHR, as well as the other MKPs that we have found to be distinctly regulated during the adipogenic conversion of 3T3-L1 cells, are warranted.

References

1. Cinti, S., The Adipose Organ, in Adipose Tissue and Adipokines in Health and Disease, G.a.M. Fantuzzi, T., Editor. 2007, Humana Press Inc.: Totowa. p. 397.
2. Cannon, B. and J. Nedergaard, Brown adipose tissue: function and physiological significance. Physiol Rev, 2004. 84(1): p. 277-359.
3. Trayhurn, P., Adipocyte biology. Obes Rev, 2007. 8 Suppl 1: p. 41-4.
4. Hausman, D.B., et al., The biology of white adipocyte proliferation. Obes Rev, 2001. 2(4): p. 239-54.
5. Spalding, K.L., et al., Dynamics of fat cell turnover in humans. Nature, 2008.
6. Bogen, B. and L. Munthe, 17.7 monocytter og makrofager, in IMMUNOLOGI. 2007, Universitetsforlaget: OSLO. p. 334.
7. Fraser, J.K., et al., Fat tissue: an underappreciated source of stem cells for biotechnology. Trends Biotechnol, 2006. 24(4): p. 150-4.
8. Rodriguez, A.M., et al., The human adipose tissue is a source of multipotent stem cells. Biochimie, 2005. 87(1): p. 125-8.
9. Avram, A.S., M.M. Avram, and W.D. James, Subcutaneous fat in normal and diseased states: 2. Anatomy and physiology of white and brown adipose tissue. J Am Acad Dermatol, 2005. 53(4): p. 671-83.
10. Miyoshi, H., et al., Control of adipose triglyceride lipase action by serine 517 of perilipin A globally regulates protein kinase A-stimulated lipolysis in adipocytes. J Biol Chem, 2007. 282(2): p. 996-1002.
11. Carmen, G.Y. and S.M. Victor, Signalling mechanisms regulating lipolysis. Cell Signal, 2006. 18(4): p. 401-8.
12. Bernlohr, D.A., N.R. Coe, and V.J. LiCata, Fatty acid trafficking in the adipocyte. Semin Cell Dev Biol, 1999. 10(1): p. 43-9.
13. Jequier, E. and L. Tappy, Regulation of body weight in humans. Physiol Rev, 1999. 79(2): p. 451-80.
14. Hanson, R.W. and L. Reshef, Glyceroneogenesis revisited. Biochimie, 2003. 85(12): p. 1199-205.
15. Badman, M.K. and J.S. Flier, The gut and energy balance: visceral allies in the obesity wars. Science, 2005. 307(5717): p. 1909-14.
16. Fernyhough, M.E., et al., PPARgamma and GLUT-4 expression as developmental regulators/markers for preadipocyte differentiation into an adipocyte. Domest Anim Endocrinol, 2007. 33(4): p. 367-78.
17. Czech, M.P., Fat targets for insulin signaling. Mol Cell, 2002. 9(4): p. 695-6.
18. Zhang, Y., et al., Positional cloning of the mouse obese gene and its human homologue. Nature, 1994. 372(6505): p. 425-32.
19. Halaas, J.L., et al., Weight-reducing effects of the plasma protein encoded by the obese gene. Science, 1995. 269(5223): p. 543-6.
20. Badman, M.K. and J.S. Flier, The adipocyte as an active participant in energy balance and metabolism. Gastroenterology, 2007. 132(6): p. 2103-15.
21. Flier, J.S., Obesity wars: molecular progress confronts an expanding epidemic. Cell, 2004. 116(2): p. 337-50.

22. Waki, H. and P. Tontonoz, Endocrine functions of adipose tissue. Annu Rev Pathol, 2007. 2: p. 31-56.
23. Kershaw, E.E. and J.S. Flier, Adipose tissue as an endocrine organ. J Clin Endocrinol Metab, 2004. 89(6): p. 2548-56.
24. Reshef, L., et al., Glyceroneogenesis and the triglyceride/fatty acid cycle. J Biol Chem, 2003. 278(33): p. 30413-6.
25. Fischer-Posovszky, P., M. Wabitsch, and Z. Hochberg, Endocrinology of adipose tissue - an update. Horm Metab Res, 2007. 39(5): p. 314-21.
26. Gustafson, B., et al., Inflamed adipose tissue: a culprit underlying the metabolic syndrome and atherosclerosis. Arterioscler Thromb Vasc Biol, 2007. 27(11): p. 2276-83.
27. Yang, Q., et al., Serum retinol binding protein 4 contributes to insulin resistance in obesity and type 2 diabetes. Nature, 2005. 436(7049): p. 356-62.
28. Fukuhara, A., et al., Visfatin: a protein secreted by visceral fat that mimics the effects of insulin. Science, 2005. 307(5708): p. 426-30.
29. Berndt, J., et al., Plasma visfatin concentrations and fat depot-specific mRNA expression in humans. Diabetes, 2005. 54(10): p. 2911-6.
30. Sandeep, S., et al., Serum visfatin in relation to visceral fat, obesity, and type 2 diabetes mellitus in Asian Indians. Metabolism, 2007. 56(4): p. 565-70.
31. Tilg, H. and A.R. Moschen, Adipocytokines: mediators linking adipose tissue, inflammation and immunity. Nat Rev Immunol, 2006. 6(10): p. 772-83.
32. Sell, H. and J. Eckel, Monocyte chemotactic protein-1 and its role in insulin resistance. Curr Opin Lipidol, 2007. 18(3): p. 258-62.
33. Fasshauer, M., et al., Monocyte chemoattractant protein 1 expression is stimulated by growth hormone and interleukin-6 in 3T3-L1 adipocytes. Biochem Biophys Res Commun, 2004. 317(2): p. 598-604.
34. Baskin, M.L., et al., Prevalence of obesity in the United States. Obes Rev, 2005. 6(1): p. 5-7.
35. Meyer, H.E. and A. Tverdal, Development of body weight in the Norwegian population. Prostaglandins Leukot Essent Fatty Acids, 2005. 73(1): p. 3-7.
36. Chen, C.M., Overview of obesity in Mainland China. Obes Rev, 2008. 9 Suppl 1: p. 14-21.
37. WHO. Obesity-definition. 2008 [cited 2008 May]; Available from: http://www.who.int/en/.
38. Kahn, S.E., R.L. Hull, and K.M. Utzschneider, Mechanisms linking obesity to insulin resistance and type 2 diabetes. Nature, 2006. 444(7121): p. 840-6.
39. Van Gaal, L.F., I.L. Mertens, and C.E. De Block, Mechanisms linking obesity with cardiovascular disease. Nature, 2006. 444(7121): p. 875-80.
40. Birmingham, C.L., et al., The cost of obesity in Canada. CMAJ, 1999. 160(4): p. 483-8.
41. Hogan, P., T. Dall, and P. Nikolov, Economic costs of diabetes in the US in 2002. Diabetes Care, 2003. 26(3): p. 917-32.
42. Gesta, S., Y.H. Tseng, and C.R. Kahn, Developmental origin of fat: tracking obesity to its source. Cell, 2007. 131(2): p. 242-56.
43. Spiegelman, B.M. and J.S. Flier, Obesity and the regulation of energy balance. Cell, 2001. 104(4): p. 531-43.

44. Wellen, K.E. and G.S. Hotamisligil, Inflammation, stress, and diabetes. J Clin Invest, 2005. 115(5): p. 1111-9.
45. Ruan, H. and H.F. Lodish, Insulin resistance in adipose tissue: direct and indirect effects of tumor necrosis factor-alpha. Cytokine Growth Factor Rev, 2003. 14(5): p. 447-55.
46. Guilherme, A., et al., Adipocyte dysfunctions linking obesity to insulin resistance and type 2 diabetes. Nat Rev Mol Cell Biol, 2008. 9(5): p. 367-77.
47. Hoene, M. and C. Weigert, The role of interleukin-6 in insulin resistance, body fat distribution and energy balance. Obes Rev, 2008. 9(1): p. 20-9.
48. Fernandez-Real, J.M. and W. Ricart, Insulin resistance and chronic cardiovascular inflammatory syndrome. Endocr Rev, 2003. 24(3): p. 278-301.
49. Berg, A.H. and P.E. Scherer, Adipose tissue, inflammation, and cardiovascular disease. Circ Res, 2005. 96(9): p. 939-49.
50. Weisberg, S.P., et al., Obesity is associated with macrophage accumulation in adipose tissue. J Clin Invest, 2003. 112(12): p. 1796-808.
51. Hotamisligil, G.S., Inflammation and metabolic disorders. Nature, 2006. 444(7121): p. 860-7.
52. Sartipy, P. and D.J. Loskutoff, Monocyte chemoattractant protein 1 in obesity and insulin resistance. Proc Natl Acad Sci U S A, 2003. 100(12): p. 7265-70.
53. Rosen, E.D. and B.M. Spiegelman, Molecular regulation of adipogenesis. Annu Rev Cell Dev Biol, 2000. 16: p. 145-71.
54. Billon, N., et al., The generation of adipocytes by the neural crest. Development, 2007. 134(12): p. 2283-92.
55. Vaananen, H.K., Mesenchymal stem cells. Ann Med, 2005. 37(7): p. 469-79.
56. Abdallah, B.M. and M. Kassem, Human mesenchymal stem cells: from basic biology to clinical applications. Gene Ther, 2008. 15(2): p. 109-16.
57. Moerman, E.J., et al., Aging activates adipogenic and suppresses osteogenic programs in mesenchymal marrow stroma/stem cells: the role of PPAR-gamma2 transcription factor and TGF-beta/BMP signaling pathways. Aging Cell, 2004. 3(6): p. 379-89.
58. Choy, L. and R. Derynck, Transforming growth factor-beta inhibits adipocyte differentiation by Smad3 interacting with CCAAT/enhancer-binding protein (C/EBP) and repressing C/EBP transactivation function. J Biol Chem, 2003. 278(11): p. 9609-19.
59. Bowers, R.R. and M.D. Lane, Wnt signaling and adipocyte lineage commitment. Cell Cycle, 2008. 7(9): p. 1191-6.
60. Farmer, S.R., Transcriptional control of adipocyte formation. Cell Metab, 2006. 4(4): p. 263-73.
61. Otto, T.C. and M.D. Lane, Adipose development: from stem cell to adipocyte. Crit Rev Biochem Mol Biol, 2005. 40(4): p. 229-42.
62. Rangwala, S.M. and M.A. Lazar, Transcriptional control of adipogenesis. Annu Rev Nutr, 2000. 20: p. 535-59.
63. Aranda, A. and A. Pascual, Nuclear hormone receptors and gene expression. Physiol Rev, 2001. 81(3): p. 1269-304.

64. Rosen, E.D. and B.M. Spiegelman, PPARgamma : a nuclear regulator of metabolism, differentiation, and cell growth. J Biol Chem, 2001. 276(41): p. 37731-4.
65. Schoonjans, K., B. Staels, and J. Auwerx, Role of the peroxisome proliferator-activated receptor (PPAR) in mediating the effects of fibrates and fatty acids on gene expression. J Lipid Res, 1996. 37(5): p. 907-25.
66. Rosen, E.D. and O.A. MacDougald, Adipocyte differentiation from the inside out. Nat Rev Mol Cell Biol, 2006. 7(12): p. 885-96.
67. Kubota, N., et al., PPAR gamma mediates high-fat diet-induced adipocyte hypertrophy and insulin resistance. Mol Cell, 1999. 4(4): p. 597-609.
68. Mueller, E., et al., Genetic analysis of adipogenesis through peroxisome proliferator-activated receptor gamma isoforms. J Biol Chem, 2002. 277(44): p. 41925-30.
69. Rosen, E.D., et al., PPAR gamma is required for the differentiation of adipose tissue in vivo and in vitro. Mol Cell, 1999. 4(4): p. 611-7.
70. Tontonoz, P., E. Hu, and B.M. Spiegelman, Stimulation of adipogenesis in fibroblasts by PPAR gamma 2, a lipid-activated transcription factor. Cell, 1994. 79(7): p. 1147-56.
71. Zhang, J., et al., Selective disruption of PPARgamma 2 impairs the development of adipose tissue and insulin sensitivity. Proc Natl Acad Sci U S A, 2004. 101(29): p. 10703-8.
72. Ramji, D.P. and P. Foka, CCAAT/enhancer-binding proteins: structure, function and regulation. Biochem J, 2002. 365(Pt 3): p. 561-75.
73. Darlington, G.J., S.E. Ross, and O.A. MacDougald, The role of C/EBP genes in adipocyte differentiation. J Biol Chem, 1998. 273(46): p. 30057-60.
74. Rosen, E.D., et al., C/EBPalpha induces adipogenesis through PPARgamma: a unified pathway. Genes Dev, 2002. 16(1): p. 22-6.
75. Linhart, H.G., et al., C/EBPalpha is required for differentiation of white, but not brown, adipose tissue. Proc Natl Acad Sci U S A, 2001. 98(22): p. 12532-7.
76. Tang, Q.Q., J.W. Zhang, and M. Daniel Lane, Sequential gene promoter interactions of C/EBPbeta, C/EBPalpha, and PPARgamma during adipogenesis. Biochem Biophys Res Commun, 2004. 319(1): p. 235-9.
77. Umek, R.M., A.D. Friedman, and S.L. McKnight, CCAAT-enhancer binding protein: a component of a differentiation switch. Science, 1991. 251(4991): p. 288-92.
78. Wu, Z., et al., Cross-regulation of C/EBP alpha and PPAR gamma controls the transcriptional pathway of adipogenesis and insulin sensitivity. Mol Cell, 1999. 3(2): p. 151-8.
79. Tang, Q.Q. and M.D. Lane, Activation and centromeric localization of CCAAT/enhancer-binding proteins during the mitotic clonal expansion of adipocyte differentiation. Genes Dev, 1999. 13(17): p. 2231-41.
80. Wu, Z., N.L. Bucher, and S.R. Farmer, Induction of peroxisome proliferator-activated receptor gamma during the conversion of 3T3 fibroblasts into adipocytes is mediated by C/EBPbeta, C/EBPdelta, and glucocorticoids. Mol Cell Biol, 1996. 16(8): p. 4128-36.

81. Wu, Z., et al., Conditional ectopic expression of C/EBP beta in NIH-3T3 cells induces PPAR gamma and stimulates adipogenesis. Genes Dev, 1995. 9(19): p. 2350-63.
82. Zuo, Y., L. Qiang, and S.R. Farmer, Activation of CCAAT/enhancer-binding protein (C/EBP) alpha expression by C/EBP beta during adipogenesis requires a peroxisome proliferator-activated receptor-gamma-associated repression of HDAC1 at the C/ebp alpha gene promoter. J Biol Chem, 2006. 281(12): p. 7960-7.
83. Zhang, J.W., et al., Role of CREB in transcriptional regulation of CCAAT/enhancer-binding protein beta gene during adipogenesis. J Biol Chem, 2004. 279(6): p. 4471-8.
84. Tang, Q.Q., T.C. Otto, and M.D. Lane, CCAAT/enhancer-binding protein beta is required for mitotic clonal expansion during adipogenesis. Proc Natl Acad Sci U S A, 2003. 100(3): p. 850-5.
85. Zhang, J.W., et al., Dominant-negative C/EBP disrupts mitotic clonal expansion and differentiation of 3T3-L1 preadipocytes. Proc Natl Acad Sci U S A, 2004. 101(1): p. 43-7.
86. Wu, J., et al., The KLF2 transcription factor does not affect the formation of preadipocytes but inhibits their differentiation into adipocytes. Biochemistry, 2005. 44(33): p. 11098-105.
87. Oishi, Y., et al., Kruppel-like transcription factor KLF5 is a key regulator of adipocyte differentiation. Cell Metab, 2005. 1(1): p. 27-39.
88. Chen, Z., et al., Krox20 stimulates adipogenesis via C/EBPbeta-dependent and -independent mechanisms. Cell Metab, 2005. 1(2): p. 93-106.
89. Birsoy, K., Z. Chen, and J. Friedman, Transcriptional Regulation of Adipogenesis by KLF4. Cell Metab, 2008. 7(4): p. 339-347.
90. Sue, N., et al., Targeted disruption of the Basic Kruppel-like Factor (Klf3) gene reveals a role in adipogenesis. Mol Cell Biol, 2008.
91. Horton, J.D., J.L. Goldstein, and M.S. Brown, SREBPs: transcriptional mediators of lipid homeostasis. Cold Spring Harb Symp Quant Biol, 2002. 67: p. 491-8.
92. Kim, J.B. and B.M. Spiegelman, ADD1/SREBP1 promotes adipocyte differentiation and gene expression linked to fatty acid metabolism. Genes Dev, 1996. 10(9): p. 1096-107.
93. Kim, J.B., et al., ADD1/SREBP1 activates PPARgamma through the production of endogenous ligand. Proc Natl Acad Sci U S A, 1998. 95(8): p. 4333-7.
94. Miard, S. and L. Fajas, Atypical transcriptional regulators and cofactors of PPARgamma. Int J Obes (Lond), 2005. 29 Suppl 1: p. S10-2.
95. Tong, Q., et al., Function of GATA transcription factors in preadipocyte-adipocyte transition. Science, 2000. 290(5489): p. 134-8.
96. Tong, Q., et al., Interaction between GATA and the C/EBP family of transcription factors is critical in GATA-mediated suppression of adipocyte differentiation. Mol Cell Biol, 2005. 25(2): p. 706-15.
97. Wolfrum, C., et al., Role of Foxa-2 in adipocyte metabolism and differentiation. J Clin Invest, 2003. 112(3): p. 345-56.

98. Wang, Y., et al., Pref-1, a preadipocyte secreted factor that inhibits adipogenesis. J Nutr, 2006. 136(12): p. 2953-6.
99. Gross, D.N., A.P. van den Heuvel, and M.J. Birnbaum, The role of FoxO in the regulation of metabolism. Oncogene, 2008. 27(16): p. 2320-36.
100. Aubert, J., N. Belmonte, and C. Dani, Role of pathways for signal transducers and activators of transcription, and mitogen-activated protein kinase in adipocyte differentiation. Cell Mol Life Sci, 1999. 56(5-6): p. 538-42.
101. Deng, J., et al., Protein inhibitor of activated STAT3 inhibits adipogenic gene expression. Biochem Biophys Res Commun, 2006. 339(3): p. 923-31.
102. Baugh, J.E., Jr., Z.E. Floyd, and J.M. Stephens, The modulation of STAT5A/GR complexes during fat cell differentiation and in mature adipocytes. Obesity (Silver Spring), 2007. 15(3): p. 583-90.
103. Floyd, Z.E. and J.M. Stephens, STAT5A promotes adipogenesis in nonprecursor cells and associates with the glucocorticoid receptor during adipocyte differentiation. Diabetes, 2003. 52(2): p. 308-14.
104. Kyriakis, J.M. and J. Avruch, Mammalian mitogen-activated protein kinase signal transduction pathways activated by stress and inflammation. Physiol Rev, 2001. 81(2): p. 807-69.
105. Pearson, G., et al., Mitogen-activated protein (MAP) kinase pathways: regulation and physiological functions. Endocr Rev, 2001. 22(2): p. 153-83.
106. Coulombe, P. and S. Meloche, Atypical mitogen-activated protein kinases: structure, regulation and functions. Biochim Biophys Acta, 2007. 1773(8): p. 1376-87.
107. Zarubin, T. and J. Han, Activation and signaling of the p38 MAP kinase pathway. Cell Res, 2005. 15(1): p. 11-8.
108. Turjanski, A.G., J.P. Vaque, and J.S. Gutkind, MAP kinases and the control of nuclear events. Oncogene, 2007. 26(22): p. 3240-53.
109. Binetruy, B., et al., Concise review: regulation of embryonic stem cell lineage commitment by mitogen-activated protein kinases. Stem Cells, 2007. 25(5): p. 1090-5.
110. Junttila, M.R., S.P. Li, and J. Westermarck, Phosphatase-mediated crosstalk between MAPK signaling pathways in the regulation of cell survival. FASEB J, 2008. 22(4): p. 954-65.
111. Davis, R.J., Signal transduction by the JNK group of MAP kinases. Cell, 2000. 103(2): p. 239-52.
112. Cuevas, B.D., A.N. Abell, and G.L. Johnson, Role of mitogen-activated protein kinase kinase kinases in signal integration. Oncogene, 2007. 26(22): p. 3159-71.
113. Raman, M., W. Chen, and M.H. Cobb, Differential regulation and properties of MAPKs. Oncogene, 2007. 26(22): p. 3100-12.
114. Benito, M., et al., Differentiation of 3T3-L1 fibroblasts to adipocytes induced by transfection of ras oncogenes. Science, 1991. 253(5019): p. 565-8.
115. Sale, E.M., P.G. Atkinson, and G.J. Sale, Requirement of MAP kinase for differentiation of fibroblasts to adipocytes, for insulin activation of p90 S6 kinase and for insulin or serum stimulation of DNA synthesis. EMBO J, 1995. 14(4): p. 674-84.

116. Camp, H.S. and S.R. Tafuri, Regulation of peroxisome proliferator-activated receptor gamma activity by mitogen-activated protein kinase. J Biol Chem, 1997. 272(16): p. 10811-6.
117. Hu, E., et al., Inhibition of adipogenesis through MAP kinase-mediated phosphorylation of PPARgamma. Science, 1996. 274(5295): p. 2100-3.
118. Tang, Q.Q., T.C. Otto, and M.D. Lane, Mitotic clonal expansion: a synchronous process required for adipogenesis. Proc Natl Acad Sci U S A, 2003. 100(1): p. 44-9.
119. Prusty, D., et al., Activation of MEK/ERK signaling promotes adipogenesis by enhancing peroxisome proliferator-activated receptor gamma (PPARgamma) and C/EBPalpha gene expression during the differentiation of 3T3-L1 preadipocytes. J Biol Chem, 2002. 277(48): p. 46226-32.
120. Tang, Q.Q., et al., Sequential phosphorylation of CCAAT enhancer-binding protein beta by MAPK and glycogen synthase kinase 3beta is required for adipogenesis. Proc Natl Acad Sci U S A, 2005. 102(28): p. 9766-71.
121. Bost, F., et al., The extracellular signal-regulated kinase isoform ERK1 is specifically required for in vitro and in vivo adipogenesis. Diabetes, 2005. 54(2): p. 402-11.
122. Bost, F., et al., The role of MAPKs in adipocyte differentiation and obesity. Biochimie, 2005. 87(1): p. 51-6.
123. Pagano, E., O. Coso, and J.C. Calvo, Down-modulation of erbB2 activity is necessary but not enough in the differentiation of 3T3-L1 preadipocytes. J Cell Biochem, 2008. 104(1): p. 274-85.
124. Engelman, J.A., M.P. Lisanti, and P.E. Scherer, Specific inhibitors of p38 mitogen-activated protein kinase block 3T3-L1 adipogenesis. J Biol Chem, 1998. 273(48): p. 32111-20.
125. Takenouchi, T., Y. Takayama, and T. Takezawa, Co-treatment with dexamethasone and octanoate induces adipogenesis in 3T3-L1 cells. Cell Biol Int, 2004. 28(3): p. 209-16.
126. Engelman, J.A., et al., Constitutively active mitogen-activated protein kinase kinase 6 (MKK6) or salicylate induces spontaneous 3T3-L1 adipogenesis. J Biol Chem, 1999. 274(50): p. 35630-8.
127. Patel, N.G., et al., Differential regulation of lipogenesis and leptin production by independent signaling pathways and rosiglitazone during human adipocyte differentiation. Diabetes, 2003. 52(1): p. 43-50.
128. Aouadi, M., et al., p38MAP Kinase activity is required for human primary adipocyte differentiation. FEBS Lett, 2007. 581(29): p. 5591-6.
129. Batchvarova, N., X.Z. Wang, and D. Ron, Inhibition of adipogenesis by the stress-induced protein CHOP (Gadd153). EMBO J, 1995. 14(19): p. 4654-61.
130. Wang, X.Z. and D. Ron, Stress-induced phosphorylation and activation of the transcription factor CHOP (GADD153) by p38 MAP Kinase. Science, 1996. 272(5266): p. 1347-9.
131. Aouadi, M., et al., Inhibition of p38MAPK increases adipogenesis from embryonic to adult stages. Diabetes, 2006. 55(2): p. 281-9.

132. Camp, H.S., S.R. Tafuri, and T. Leff, c-Jun N-terminal kinase phosphorylates peroxisome proliferator-activated receptor-gamma1 and negatively regulates its transcriptional activity. Endocrinology, 1999. 140(1): p. 392-7.
133. Hirosumi, J., et al., A central role for JNK in obesity and insulin resistance. Nature, 2002. 420(6913): p. 333-6.
134. Jaeschke, A., M.P. Czech, and R.J. Davis, An essential role of the JIP1 scaffold protein for JNK activation in adipose tissue. Genes Dev, 2004. 18(16): p. 1976-80.
135. Sharma, G. and M.L. Goalstone, Dominant negative FTase (DNFTalpha) inhibits ERK5, MEF2C and CREB activation in adipogenesis. Mol Cell Endocrinol, 2005. 245(1-2): p. 93-104.
136. Alonso, A., et al., Protein tyrosine phosphatases in the human genome. Cell, 2004. 117(6): p. 699-711.
137. Jeffrey, K.L., et al., Targeting dual-specificity phosphatases: manipulating MAP kinase signalling and immune responses. Nat Rev Drug Discov, 2007. 6(5): p. 391-403.
138. Farooq, A. and M.M. Zhou, Structure and regulation of MAPK phosphatases. Cell Signal, 2004. 16(7): p. 769-79.
139. Kondoh, K. and E. Nishida, Regulation of MAP kinases by MAP kinase phosphatases. Biochim Biophys Acta, 2007. 1773(8): p. 1227-37.
140. Zhang, Y. and C. Dong, Regulatory mechanisms of mitogen-activated kinase signaling. Cell Mol Life Sci, 2007. 64(21): p. 2771-89.
141. Dickinson, R.J. and S.M. Keyse, Diverse physiological functions for dual-specificity MAP kinase phosphatases. J Cell Sci, 2006. 119(Pt 22): p. 4607-15.
142. Keyse, S.M., Dual-specificity MAP kinase phosphatases (MKPs) and cancer. Cancer Metastasis Rev, 2008. 27(2): p. 253-61.
143. Wang, X. and Y. Liu, Regulation of innate immune response by MAP kinase phosphatase-1. Cell Signal, 2007. 19(7): p. 1372-82.
144. Chi, H., et al., Dynamic regulation of pro- and anti-inflammatory cytokines by MAPK phosphatase 1 (MKP-1) in innate immune responses. Proc Natl Acad Sci U S A, 2006. 103(7): p. 2274-9.
145. Hammer, M., et al., Dual specificity phosphatase 1 (DUSP1) regulates a subset of LPS-induced genes and protects mice from lethal endotoxin shock. J Exp Med, 2006. 203(1): p. 15-20.
146. Christie, G.R., et al., The dual-specificity protein phosphatase DUSP9/MKP-4 is essential for placental function but is not required for normal embryonic development. Mol Cell Biol, 2005. 25(18): p. 8323-33.
147. Dickinson, R.J., et al., Expression of the ERK-specific MAP kinase phosphatase PYST1/MKP3 in mouse embryos during morphogenesis and early organogenesis. Mech Dev, 2002. 113(2): p. 193-6.
148. Li, C., et al., Dusp6 (Mkp3) is a negative feedback regulator of FGF-stimulated ERK signaling during mouse development. Development, 2007. 134(1): p. 167-76.
149. Rechsteiner, M. and S.W. Rogers, PEST sequences and regulation by proteolysis. Trends Biochem Sci, 1996. 21(7): p. 267-71.

150. Liu, Y., E.G. Shepherd, and L.D. Nelin, MAPK phosphatases--regulating the immune response. Nat Rev Immunol, 2007. 7(3): p. 202-12.
151. Martell, K.J., et al., hVH-5: a protein tyrosine phosphatase abundant in brain that inactivates mitogen-activated protein kinase. J Neurochem, 1995. 65(4): p. 1823-33.
152. Bernabeu, R., G. Di Scala, and J. Zwiller, Odor regulates the expression of the mitogen-activated protein kinase phosphatase gene hVH-5 in bilateral entorhinal cortex-lesioned rats. Brain Res Mol Brain Res, 2000. 75(1): p. 113-20.
153. Thiriet, N., et al., Cocaine and fluoxetine induce the expression of the hVH-5 gene encoding a MAP kinase phosphatase. Brain Res Mol Brain Res, 1998. 62(2): p. 150-7.
154. Ishibashi, T., et al., Expression cloning of a human dual-specificity phosphatase. Proc Natl Acad Sci U S A, 1992. 89(24): p. 12170-4.
155. Alonso, A., et al., Inhibitory role for dual specificity phosphatase VHR in T cell antigen receptor and CD28-induced Erk and Jnk activation. J Biol Chem, 2001. 276(7): p. 4766-71.
156. Alonso, A., et al., Tyrosine phosphorylation of VHR phosphatase by ZAP-70. Nat Immunol, 2003. 4(1): p. 44-8.
157. Kang, T.H. and K.T. Kim, Negative regulation of ERK activity by VRK3-mediated activation of VHR phosphatase. Nat Cell Biol, 2006. 8(8): p. 863-9.
158. Rahmouni, S., et al., Loss of the VHR dual-specific phosphatase causes cell-cycle arrest and senescence. Nat Cell Biol, 2006. 8(5): p. 524-31.
159. Marti, F., et al., Negative-feedback regulation of CD28 costimulation by a novel mitogen-activated protein kinase phosphatase, MKP6. J Immunol, 2001. 166(1): p. 197-206.
160. Bazuine, M., et al., Mitogen-activated protein kinase (MAPK) phosphatase-1 and -4 attenuate p38 MAPK during dexamethasone-induced insulin resistance in 3T3-L1 adipocytes. Mol Endocrinol, 2004. 18(7): p. 1697-707.
161. Sakaue, H., et al., Role of MAPK phosphatase-1 (MKP-1) in adipocyte differentiation. J Biol Chem, 2004. 279(38): p. 39951-7.
162. Schliess, F., A.K. Kurz, and D. Haussinger, Glucagon-induced expression of the MAP kinase phosphatase MKP-1 in rat hepatocytes. Gastroenterology, 2000. 118(5): p. 929-36.
163. Kassel, O., et al., Glucocorticoids inhibit MAP kinase via increased expression and decreased degradation of MKP-1. EMBO J, 2001. 20(24): p. 7108-16.
164. Kusari, A.B., et al., Insulin-induced mitogen-activated protein (MAP) kinase phosphatase-1 (MKP-1) attenuates insulin-stimulated MAP kinase activity: a mechanism for the feedback inhibition of insulin signaling. Mol Endocrinol, 1997. 11(10): p. 1532-43.
165. Wu, J.J., et al., Mice lacking MAP kinase phosphatase-1 have enhanced MAP kinase activity and resistance to diet-induced obesity. Cell Metab, 2006. 4(1): p. 61-73.
166. Xu, H., et al., Dual specificity mitogen-activated protein (MAP) kinase phosphatase-4 plays a potential role in insulin resistance. J Biol Chem, 2003. 278(32): p. 30187-92.

167. Ito, A., et al., Role of MAPK phosphatase-1 in the induction of monocyte chemoattractant protein-1 during the course of adipocyte hypertrophy. J Biol Chem, 2007. 282(35): p. 25445-52.
168. Clontech Laboratories, I. RevTet System User Manual. [pdf document] 2004 19 February 2004 [cited 2008 June]; Available from: http://www.clontech.com/images/pt/dis_manuals/PT3223-1.pdf.
169. Pear, W.S., et al., Production of high-titer helper-free retroviruses by transient transfection. Proc Natl Acad Sci U S A, 1993. 90(18): p. 8392-6.
170. Gossen, M., et al., Transcriptional activation by tetracyclines in mammalian cells. Science, 1995. 268(5218): p. 1766-9.
171. Urlinger, S., et al., Exploring the sequence space for tetracycline-dependent transcriptional activators: novel mutations yield expanded range and sensitivity. Proc Natl Acad Sci U S A, 2000. 97(14): p. 7963-8.
172. Gossen, M. and H. Bujard, Tight control of gene expression in mammalian cells by tetracycline-responsive promoters. Proc Natl Acad Sci U S A, 1992. 89(12): p. 5547-51.
173. Yan, W., W. Chen, and L. Huang, Mechanism of adjuvant activity of cationic liposome: phosphorylation of a MAP kinase, ERK and induction of chemokines. Mol Immunol, 2007. 44(15): p. 3672-81.
174. Todd, J.L., et al., Dual-specificity protein tyrosine phosphatase VHR down-regulates c-Jun N-terminal kinase (JNK). Oncogene, 2002. 21(16): p. 2573-83.
175. Todd, J.L., K.G. Tanner, and J.M. Denu, Extracellular regulated kinases (ERK) 1 and ERK2 are authentic substrates for the dual-specificity protein-tyrosine phosphatase VHR. A novel role in down-regulating the ERK pathway. J Biol Chem, 1999. 274(19): p. 13271-80.
176. Moldes, M., et al., Peroxisome-proliferator-activated receptor gamma suppresses Wnt/beta-catenin signalling during adipogenesis. Biochem J, 2003. 376(Pt 3): p. 607-13.
177. Stuke, A.W. and A. Strom, Tetracycline-regulated highly inducible expression of the human prion protein in murine 3T3 cells. Protein Expr Purif, 2005. 39(1): p. 8-17.
178. Orlicky, D.J., J. DeGregori, and J. Schaack, Construction of stable coxsackievirus and adenovirus receptor-expressing 3T3-L1 cells. J Lipid Res, 2001. 42(6): p. 910-5.
179. Ross, S.A., et al., Efficient adenovirus transduction of 3T3-L1 adipocytes stably expressing coxsackie-adenovirus receptor. Biochem Biophys Res Commun, 2003. 302(2): p. 354-8.